with dependable DABG *P*-values. Inclusion of these probe sets increases the standard deviation and decreases the *DV* of the aberrantly spliced exon.

Potential roles of novel aberrant splicing events in DM1

In this study, we identified 27 DM1-specific aberrant splicing, in which 25 have not been published yet. Among the 25 exons, aberrant splicing events of two exons were 'uniquely' observed in DM1: one is inclusion of the LIM domain binding 3 (*LDB3*) exon 4 and the other is inclusion of titin (*TTN*) exon 45. Interestingly, both encode structural proteins of muscle fiber.

LDB3, also known as Cypher/ZASP (Z-band alternatively spliced PDZ-motif protein), contains a PDZ domain at the N-terminus and one or three LIM domains at the C-terminus. LDB3 is localized to the Z-line and interacts with α-actinin 2 through its PDZ-domain and with protein kinase C via its C-terminal LIM domains.[28] LDB3 is likely to have an essential role in supporting Z-line structure and muscle function during contraction.[29] *LDB3* has several isoforms. As inclusion of exon 4 is preferentially observed in the fetal heart,[30] the aberrant inclusion of exon 4 in the skeletal muscles in DM1 would lead to dysfunction or morphological abnormalities of muscle fiber. Recently, phosphoglucomutase 1 (PGM1), an enzyme involved in glycolysis and gluconeogenesis, has been known to bind to the domain encoded by exon 4 of *LDB3*. *LDB3* mutations in exon 4 reduce the binding to PGM1 and develop dilated cardiomyopathy.[31] On the other hand, the increased binding of PGM1 and LDB3 through aberrant inclusion of exon 4 might be involved in the pathogenesis of muscle atrophy, weakness and histological abnormalities in DM1.

TTN encodes the largest protein in mammals and the third most abundant protein in muscle.[32] An N-terminal Z-disc region and a C-terminal M-line region bind to the Z-line and M-line of the sarcomere, respectively, so that a single molecule extends half the length of a sarcomere. Titin is critically important for myofibril elasticity and structural integrity. Its elasticity lies specifically in the I-band region and contains two elements in series with different properties: the tandem immunoglobulin (Ig) and PEVK domains.[33] Different *TTN* isoforms contribute to differences in elasticity of different muscle types.[34] As exon 45 is located at the tandem Ig domains, aberrant inclusion of exon 45 in DM1 might lead to defective myofibril assembly and function.

ACKNOWLEDGEMENTS

This work was supported by Grants-in-Aid from the Ministry of Education, Culture, Sports, Science and Technology as well as the Ministry of Health, Labor and Welfare of Japan.

1 Wang, E. T., Sandberg, R., Luo, S., Khrebtukova, I., Zhang, L., Mayr, C. *et al.* Alternative isoform regulation in human tissue transcriptomes. *Nature* **456,** 470–476 (2008).
2 Pan, Q., Shai, O., Lee, L. J., Frey, B. J. & Blencowe, B. J. Deep surveying of alternative splicing complexity in the human transcriptome by high-throughput sequencing. *Nat. Genet.* **40,** 1413–1415 (2008).
3 Smith, C. W. & Valcarcel, J. Alternative pre-mRNA splicing: the logic of combinatorial control. *Trends Biochem. Sci.* **25,** 381–388 (2000).
4 Caceres, J. F. & Kornblihtt, A. R. Alternative splicing: multiple control mechanisms and involvement in human disease. *Trends Genet.* **18,** 186–193 (2002).
5 O'Rourke, J. R. & Swanson, M. S. Mechanisms of RNA-mediated disease. *J. Biol. Chem.* **284,** 7419–7423 (2009).
6 Cooper, T. A., Wan, L. & Dreyfuss, G. RNA and disease. *Cell* **136,** 777–793 (2009).
7 Harper, P. S. & Monckton, D. G. in *Myology* 3rd edn (ed. Engel, A. G.) Vol. 2, 1039–1076 (McGraw-Hill, New York, 2004).
8 Aslanidis, C., Jansen, G., Amemiya, C., Shutler, G., Mahadevan, M., Tsilfidis, C. *et al.* Cloning of the essential myotonic dystrophy region and mapping of the putative defect. *Nature* **355,** 548–551 (1992).
9 Brook, J. D., McCurrach, M. E., Harley, H. G., Buckler, A. J., Church, D., Aburatani, H. *et al.* Molecular basis of myotonic dystrophy: expansion of a trinucleotide (CTG) repeat at the 3′ end of a transcript encoding a protein kinase family member. *Cell* **68,** 799–808 (1992).
10 Buxton, J., Shelbourne, P., Davies, J., Jones, C., Van Tongeren, T., Aslanidis, C. *et al.* Detection of an unstable fragment of DNA specific to individuals with myotonic dystrophy. *Nature* **355,** 547–548 (1992).
11 Liquori, C. L., Ricker, K., Moseley, M. L., Jacobsen, J. F., Kress, W., Naylor, S. L. *et al.* Myotonic dystrophy type 2 caused by a CCTG expansion in intron 1 of ZNF9. *Science* **293,** 864–867 (2001).
12 Gharehbaghi-Schnell, E. B., Finsterer, J., Korschineck, I., Mamoli, B. & Binder, B. R. Genotype-phenotype correlation in myotonic dystrophy. *Clin. Genet.* **53,** 20–26 (1998).
13 Consortium T. I. M. D. New nomenclature and DNA testing guidelines for myotonic dystrophy type 1 (DM1). *Neurology* **54,** 1218–1221 (2000).
14 Saito, T., Amakusa, Y., Kimura, T., Yahara, O., Aizawa, H., Ikeda, Y. *et al.* Myotonic dystrophy type 2 in Japan: ancestral origin distinct from Caucasian families. *Neurogenetics* **9,** 61–63 (2008).
15 Osborne, R. J., Lin, X., Welle, S., Sobczak, K., O'Rourke, J. R., Swanson, M. S. *et al.* Transcriptional and post-transcriptional impact of toxic RNA in myotonic dystrophy. *Hum. Mol. Genet.* **18,** 1471–1481 (2009).
16 Wang, G. S., Kearney, D. L., De Biasi, M., Taffet, G. & Cooper, T. A. Elevation of RNA-binding protein CUGBP1 is an early event in an inducible heart-specific mouse model of myotonic dystrophy. *J. Clin. Invest.* **117,** 2802–2811 (2007).
17 Kuyumcu-Martinez, N. M., Wang, G. S. & Cooper, T. A. Increased steady-state levels of CUGBP1 in myotonic dystrophy 1 are due to PKC-mediated hyperphosphorylation. *Mol. Cell* **28,** 68–78 (2007).
18 Nezu, Y., Kino, Y., Sasagawa, N., Nishino, I. & Ishiura, S. Expression of MBNL and CELF mRNA transcripts in muscles with myotonic dystrophy. *Neuromuscul. Disord.* **17,** 306–312 (2007).
19 Thornton, C. A., Johnson, K. & Moxley, 3rd R. T. Myotonic dystrophy patients have larger CTG expansions in skeletal muscle than in leukocytes. *Ann. Neurol.* **35,** 104–107 (1994).
20 Srinivasan, K., Shiue, L., Hayes, J. D., Centers, R., Fitzwater, S., Loewen, R. *et al.* Detection and measurement of alternative splicing using splicing-sensitive microarrays. *Methods* **37,** 345–359 (2005).
21 Lin, X., Miller, J. W., Mankodi, A., Kanadia, R. N., Yuan, Y., Moxley, R. T. *et al.* Failure of MBNL1-dependent post-natal splicing transitions in myotonic dystrophy. *Hum. Mol. Genet.* **15,** 2087–2097 (2006).
22 Orengo, J. P., Ward, A. J. & Cooper, T. A. Alternative splicing dysregulation secondary to skeletal muscle regeneration. *Ann. Neurol.* **69,** 681–690 (2011).
23 Fugier, C., Klein, A. F., Hammer, C., Vassilopoulos, S., Ivarsson, Y., Toussaint, A. *et al.* Misregulated alternative splicing of BIN1 is associated with T tubule alterations and muscle weakness in myotonic dystrophy. *Nat. Med.* **17,** 720–725 (2011).
24 Sharma, A., Markey, M., Torres-Munoz, K., Varia, S., Kadakia, M., Bubulya, A. *et al.* Son maintains accurate splicing for a subset of human pre-mRNAs. *J. Cell Sci.* **124,** 4286–4298 (2011).
25 Chang, J. G., Yang, D. M., Chang, W. H., Chow, L. P., Chan, W. L., Lin, H. H. *et al.* Small molecule amiloride modulates oncogenic RNA alternative splicing to devitalize human cancer cells. *PloS One* **6,** e18643 (2011).
26 Dutertre, M., Sanchez, G., De Cian, M. C., Barbier, J., Dardenne, E., Gratadou, L. *et al.* Cotranscriptional exon skipping in the genotoxic stress response. *Nat. Struct. Mol. Biol.* **17,** 1358–1366 (2010).
27 Kalsotra, A., Xiao, X., Ward, A. J., Castle, J. C., Johnson, J. M., Burge, C. B. *et al.* A postnatal switch of CELF and MBNL proteins reprograms alternative splicing in the developing heart. *Proc. Natl Acad. Sci. USA* **105,** 20333–20338 (2008).
28 Zhou, Q., Ruiz-Lozano, P., Martone, M. E. & Chen, J. Cypher, a striated muscle-restricted PDZ and LIM domain-containing protein, binds to alpha-actinin-2 and protein kinase C. *J. Biol. Chem.* **274,** 19807–19813 (1999).
29 Zhou, Q., Chu, P. H., Huang, C., Cheng, C. F., Martone, M. E., Knoll, G. *et al.* Ablation of Cypher, a PDZ-LIM domain Z-line protein, causes a severe form of congenital myopathy. *J. Cell. Biol.* **155,** 605–612 (2001).
30 Huang, C., Zhou, Q., Liang, P., Hollander, M. S., Sheikh, F., Li, X. *et al.* Characterization and *in vivo* functional analysis of splice variants of cypher. *J. Biol. Chem.* **278,** 7360–7365 (2003).
31 Arimura, T., Inagaki, N., Hayashi, T., Shichi, D., Sato, A., Hinohara, K. *et al.* Impaired binding of ZASP/Cypher with phosphoglucomutase 1 is associated with dilated cardiomyopathy. *Cardiovasc. Res.* **83,** 80–88 (2009).
32 Gregorio, C. C., Granzier, H., Sorimachi, H. & Labeit, S. Muscle assembly: a titanic achievement? *Curr. Opin. Cell Biol.* **11,** 18–25 (1999).
33 Horowits, R. The physiological role of titin in striated muscle. *Rev. Physiol. Biochem. Pharmacol.* **138,** 57–96 (1999).
34 Freiburg, A., Trombitas, K., Hell, W., Cazorla, O., Fougerousse, F., Centner, T. *et al.* Series of exon-skipping events in the elastic spring region of titin as the structural basis for myofibrillar elastic diversity. *Circ. Res.* **86,** 1114–1121 (2000).

Supplementary Information accompanies the paper on Journal of Human Genetics website (http://www.nature.com/jhg)

Neuron
Article

Dlx1&2-Dependent Expression of *Zfhx1b (Sip1, Zeb2)* Regulates the Fate Switch between Cortical and Striatal Interneurons

Gabriel L. McKinsey,[1,2] Susan Lindtner,[1] Brett Trzcinski,[3] Axel Visel,[4,5] Len A. Pennacchio,[4,5] Danny Huylebroeck,[6] Yujiro Higashi,[7] and John L.R. Rubenstein[1,*]
[1]Department of Psychiatry, Neuroscience Program, and the Nina Ireland Laboratory of Developmental Neurobiology
[2]Neuroscience Graduate Program
University of California, San Francisco (UCSF), San Francisco, CA 94158-2324, USA
[3]University of Michigan Medical School, Ann Arbor, MI 48109-2026, USA
[4]Genomics Division, MS 84-171, Lawrence Berkeley National Laboratory, Berkeley, CA 94720, USA
[5]U.S. Department of Energy Joint Genome Institute, Walnut Creek, CA 94598, USA
[6]Laboratory of Molecular Biology (Celgen), Department of Development and Regeneration, University of Leuven, 3000 Leuven, Belgium
[7]Department of Perinatology, Institute for Developmental Research, Aichi Human Service Center, Kasugai, Aichi 480-0392, Japan
*Correspondence: john.rubenstein@ucsf.edu
http://dx.doi.org/10.1016/j.neuron.2012.11.035

SUMMARY

Mammalian pallial (cortical and hippocampal) and striatal interneurons are both generated in the embryonic subpallium, including the medial ganglionic eminence (MGE). Herein we demonstrate that the *Zfhx1b (Sip1, Zeb2)* zinc finger homeobox gene is required in the MGE, directly downstream of *Dlx1&2*, to generate cortical interneurons that express *Cxcr7*, *MafB*, and *cMaf*. In its absence, *Nkx2-1* expression is not repressed, and cells that ordinarily would become cortical interneurons appear to transform toward a subtype of GABAergic striatal interneurons. These results show that *Zfhx1b* is required to generate cortical interneurons, and suggest a mechanism for the epilepsy observed in humans with *Zfhx1b* mutations (Mowat-Wilson syndrome).

INTRODUCTION

Cell type specification within the embryonic basal ganglia is regulated at multiple levels. Distinct subdivisions within this region generate distinct neurons. For instance, the lateral ganglionic eminence (LGE) generates striatal projection neurons whereas the medial ganglionic eminence (MGE) generates pallidal projection neurons. Domains within the MGE are biased toward generating different cell types, whereas the rostrodorsal MGE largely produces cortical and striatal interneurons, the caudoventral MGE largely produces pallidal projection neurons (Flandin et al., 2010; Nobrega-Pereira et al., 2010). Distinct MGE-derived cortical interneuron subtypes appear to be generated from the same progenitors, perhaps in a temporal sequence (Brown et al., 2011).

Cortical and striatal interneurons are both generated from the MGE (Marin et al., 2000). The *Nkx2-1* homeobox transcription factor has a central role in specifying their identity. While *Nkx2-1* is initially required for both of these cell types, *Nkx2-1* expression is repressed soon after immature cortical interneurons tangentially migrate from the MGE, while it is maintained in striatal interneurons (Butt et al., 2008; Marin et al., 2000; Nóbrega-Pereira et al., 2008; Sussel et al., 1999).

Forced expression of *Nkx2-1* in cortical interneurons changes their migration so that they settle in the striatum (Nóbrega-Pereira et al., 2008), providing additional evidence that repression of *Nkx2-1* is a key step in generating cortical interneurons. How *Nkx2-1* expression is repressed in these cells is unknown.

Herein, we provide evidence that the *Zfhx1b* (*Sip1*, *Zeb2*) zinc-finger homeobox transcription factor is required to repress *Nkx2-1* in the generation of cortical interneurons. In its absence, we find a decrease in cortical interneurons concomitant with increased striatal *nNOS/NPY/Sst* GABAergic interneurons. We provide evidence that expression of the *cMaf* transcription factor is a highly specific marker of the cortical interneuron lineage, and discovered that its expression is lost in *Zfhx1b* mutants.

Previous analysis of *Zfhx1b* mouse mutants has shed light on its functions in the development of cortical projection neurons (Miquelajauregui et al., 2007; Seuntjens et al., 2009). In humans, mutations of *Zfhx1b* result in Mowat-Wilson syndrome, a developmental disorder characterized by mental retardation, epilepsy, and defects of neural crest-derived tissues, including craniofacial and enteric nervous system (Mowat et al., 2003). Our results that demonstrate *Zfhx1b* is required to generate cortical interneurons suggest a mechanism for the epilepsy observed in Mowat-Wilson syndrome.

RESULTS

Conditional Deletion of *Zfhx1b* in the VZ or the SVZ of the Subpallium using *Nkx2.1-Cre* or *Dlx12b-Cre*

Zfhx1b prenatal expression has been noted in migrating cortical interneurons and the subpallial telencephalon (Batista-Brito et al., 2008; Seuntjens et al., 2009). We found that *Zfhx1b* RNA is expressed in E12.5 MGE-derived cells that are tangentially

migrating through the LGE and into the cortex by performing fluorescent in situ hybridization (FISH) on a brain in which MGE-derived cells expressed EGFP (expressed due to *Nkx2.1-Cre* induced recombination of the *CAG:CAT-EGFP* Cre reporter allele) (see Figures S1A–S1A″ available online).

To determine the role of *Zfhx1b* in the development of the basal ganglia, we used a conditional mutagenesis approach. Using an allele of *Zfhx1b*, in which exon 7 is floxed (Higashi et al., 2002), we removed *Zfhx1b* expression using two different Cre alleles. Deletion of exon 7 creates a frameshift mutation and premature truncation of the protein. Previous analysis failed to detect the truncated mutant protein in *Zfhx1b* mutant tissues, providing evidence that this is a null allele (Higashi et al., 2002).

To remove *Zfhx1b* in the early progenitors of the MGE, we used the *Nkx2.1-Cre* allele (Xu et al., 2008), which drives Cre expression in the ventricular zone (VZ) of the MGE beginning around E9.5 (later it also drives expression in the subventricular and mantle zones [SVZ and MZ]). To differentiate between the role of *Zfhx1b* in the VZ and the SVZ/MZ, we used the *Dlx1/2b-Cre* allele (Potter et al., 2008), which drives Cre expression in the SVZ and MZ of the entire subpallium beginning around E10.5. To examine the pattern of recombination, we used an antisense riboprobe designed against *Zfhx1b* exon 7.

By E12.5, Cre activity from both the *Nkx2.1-Cre* and *Dlx1/2b-Cre* alleles removed *Zfhx1b* RNA expression in the expected patterns (Figures 1A–1C). As previously reported, the *Nkx2-1* allele did not express Cre in the dorsal-most portion of the MGE, thus explaining the persistence of *Zfhx1b* in that location (Figure 1B). Of note, in the *Nkx2.1-Cre; Zfhx1b* conditional mutant brains, *Zfhx1b* RNA expression was not observed in the cells that appear to be migrating from the dorsal MGE into the mantle of the LGE, suggesting that the *Zfhx1b*$^+$ cells in the mantle of the E12.5 LGE are likely to be MGE-derived cells (e.g., cortical and/or striatal interneurons) (X in Figure 1B). Also, note that *Dlx1/2b-Cre* leads to recombination in the SVZ and MZ of the LGE, MGE and CGE (white arrowhead, Figure 1C, and data not shown).

Next, we examined the expression of *Zfhx1b*'s closely related homolog, *Zfhx1a*, in the E12.5 control and mutant telencephalon. Both *Zfhx1a* and *Zfhx1b* are expressed in the subpallial VZ, whereas only *Zfhx1b* is clearly expressed in the SVZ (Figures 1A and S1B). *Zfhx1a*'s expression did not clearly change in the *Nkx2.1-Cre* mediated *Zfhx1b* mutant (Figures S1B–S1S1D′). Thus, in the *Nkx2.1-Cre* conditional *Zfhx1b* mutant, only the VZ of the MGE continued to strongly express a *Zfhx* homolog.

MGE-Derived Pallial Interneurons Migrate to the Striatum When Deleting *Zfhx1b* in the VZ of the MGE using *Nkx2.1-Cre*

We analyzed the effect of deleting *Zfhx1b*, using *Nkx2.1-Cre* at multiple developmental stages, including E12.5, E15.5, and P0. To track the fate of *Zfhx1b* mutant cells, we used the *CAG:CAT-EGFP* Cre reporter allele (Kawamoto et al., 2000). Mutant brains had the following genotype: *Nkx2.1-Cre;Zfhx1b*$^{F/-}$*;CAG:CAT-EGFP;* whereas controls had the following genotype: *Nkx2.1-Cre;Zfhx1b*$^{F/+}$*;CAG:CAT-EGFP* (on occasion, some were: *Nkx2.1-Cre; Zfhx1b*$^{F/+}$). At E12.5, while the control brain showed a robust stream of EGFP$^+$ cells migrating into the cortex, the mutant's EGFP$^+$ MGE derivatives failed to migrate to the cortex, and many were detected in the LGE mantle (Figures 1D–1G′).

Next, we analyzed the phenotype using molecular markers of MGE-derived cells including *Nkx2-1* and *Lhx6*. While *Nkx2-1* RNA and protein is expressed throughout the VZ and SVZ of the MGE, its expression thereafter is restricted to specific neuronal lineages. MGE-derived cortical interneurons repress *Nkx2.1* expression as they migrate out of the MGE while most, but not all, classes of striatal interneurons maintain *Nkx2.1* expression. (Flandin et al., 2010; Marin et al., 2000; Nóbrega-Pereira et al., 2008; Sussel et al., 1999). In the mutants, there was a subtle increase in *Nkx2-1* RNA expression in the LGE and CGE (Figures 1H–1J′). This increase was more apparent at higher magnification when analyzing NKX2-1 protein expression (Figures 1G and 1G′) and at later stages (E13.5 and E15.5) (Figures 1N–1P′ and 2A–2F′).

EGFP and NKX2-1 protein expression in control brains colocalized in a subset of cells derived from the MGE. EGFP/NKX2-1$^+$ cells were observed in the MGE VZ and SVZ progenitors and a subset of their derived neurons, including the globus pallidus, and striatal interneurons (Xu et al., 2008; Figure 1G, solid arrowheads), while interneurons migrating to the cerebral cortex showed little to no NKX2-1 protein expression (Figure 1G, open arrowheads). In mutant brains, however, most if not all EGFP labeled cells had detectable levels of NKX2-1 protein, with many cells strongly coexpressing NKX2-1 and EGFP in the LGE MZ, and in a region lateral to the globus pallidus (Figure 1G′, solid arrowheads). Thus, *Zfhx1b* mutants had a defect in their ability to repress *Nkx2-1* RNA and protein expression, concomitant with failure of MGE-derived migration to the cerebral cortex. While *Zfhx1b* was required to repress *Nkx2-1* expression, we did not find evidence that *Nkx2-1* regulated *Zfhx1b* expression; this conclusion was based on in situ hybridization analysis of *Zfhx1b* expression in mice lacking *Nkx2-1* in newly born MGE neurons at E15.5 (*Nkx2-1* conditional mutant with *Dlx5/6-Cre*) (Figure S6).

Lhx6 RNA is expressed in tangentially migrating cells that are immature cortical and striatal interneurons, as well as cell types that remain in the subpallium (Flandin et al., 2011; Lavdas et al., 1999; Liodis et al., 2007; Sussel et al., 1999; Zhao et al., 2008). In the *Zfhx1b* mutant, *Lhx6*$^+$ cells failed to be detected in the pallium, whereas they continued to be densely located throughout the MGE, and as a scattered population in the LGE and CGE (Figures 1K–1M′). On the other hand, *Lhx8* and *Gbx2* RNA expression was not appreciably changed in the mutants (Figures S1H–S1J′). Thus, Zfhx1b mutants may have a selective defect in cells fated to become pallial interneurons, but not cholinergic striatal interneurons. To explore this hypothesis we studied the phenotype at later developmental stages.

By E15.5, the tangential migration of immature cortical interneurons can be readily visualized by expression of *Lhx6*, *Somatostatin* (*Sst*), and EGFP (in *Nkx2.1-Cre;CAG-EGFP* brains) (Figures 2 and S2D–S2F). By contrast, in *Zfhx1b* mutants (*Nkx2.1-Cre*), pallial expression of *Lhx6*, *Sst*, and EGFP was strongly attenuated (Figures 2 and S2D′–S2F′). On the other hand, subpallial expression of these markers was increased in two locations: the striatum (asterisks, Figures 2A–2C′, 2G–2I′,

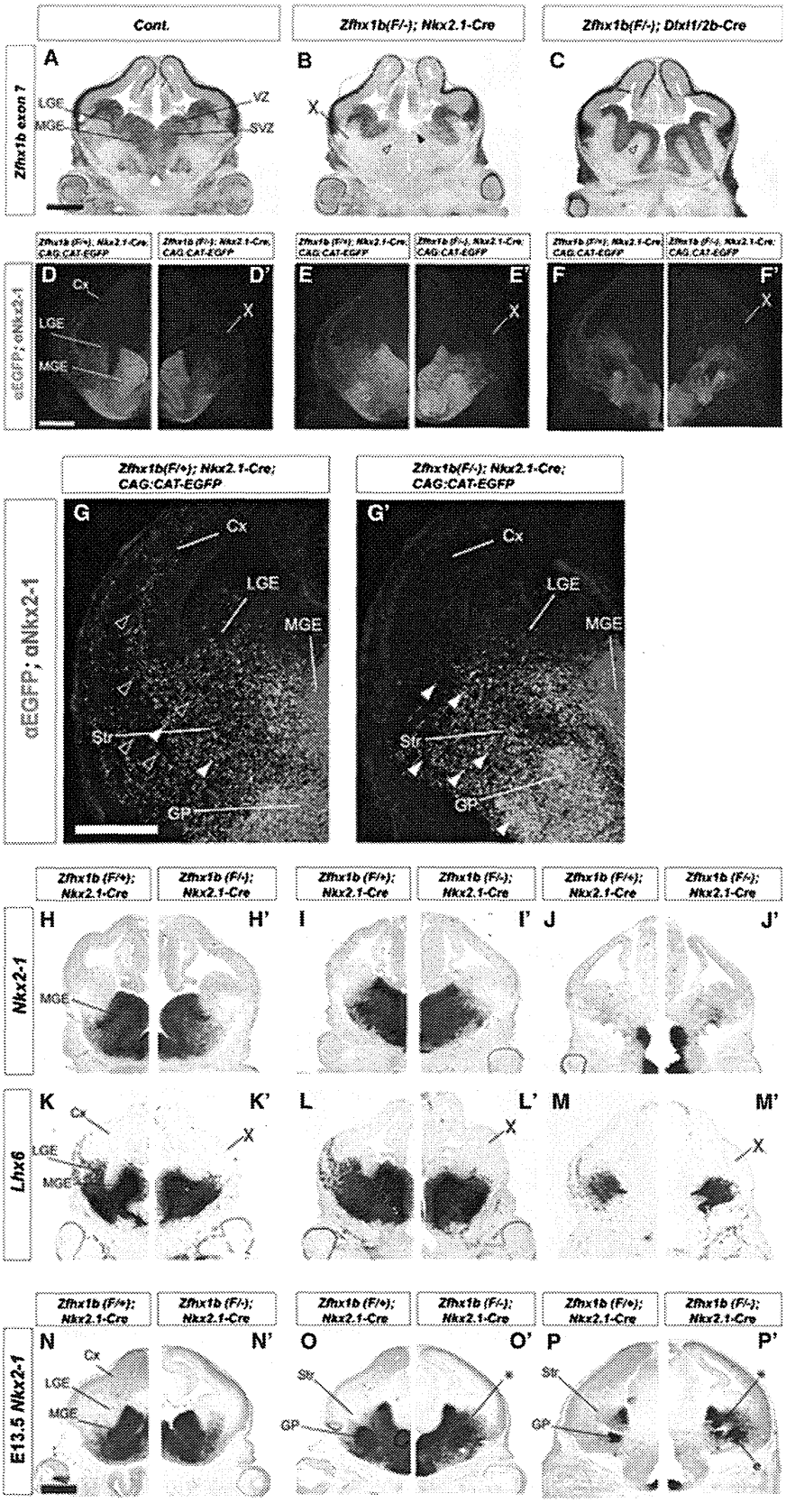

Figure 1. *Zfhx1b* Expression in the MGE Is Required for Interneuron Migration at E12.5

(A–C) *Zfhx1b* RNA expression detected by in situ hybridization in control and conditional *Zfhx1b* mutant telencephalons. (B) *Nkx2.1-Cre*. (C) *Dlxi12b-Cre*. Black arrowhead in (B) shows loss of *Zfhx1b* expression in the MGE VZ (except dorsal-most MGE). White arrowheads in (B) and (C) show loss of Zfhx1b expression in the SVZ of the MGE. X in (B) shows loss of *Zfhx1b* expression in the SVZ/MZ of the LGE. (D–P′) Coronal hemisections of the telencephalon comparing gene expression in three rostral-to-caudal planes of section in control (left side) and *Zfhx1b Nkx2.1-Cre* conditional mutants (right side). (D–F′) Two color immunofluoresence detection of EGFP (green) and NKX2-1 (red). (G and G′) Higher magnification view of two color immunofluoresence detection of EGFP (green) and Nkx2-1 (red) in control (G) and *Zfhx1b* mutant (G′). Solid white arrowheads show increased numbers of cells that express both EGFP (green) and NKX2-1 (red) in the mutant's LGE/Str. In the wild-type cortex, black arrowheads (with white outline) show that cells express EGFP (green) and not NKX2-1. (H–P′) In situ hybridization expression analysis at E12.5 of *Nkx2-1* (H–J′) and *Lhx6* (K–M′), and at E13.5 of *Nkx2-1* (N–P′). Asterisks in (N)–(P′) show increased numbers of labeled cells in striatum. X in (K′)–(M–) notes the loss of labeled cells in the cortex.

Abbreviations: Cx, cortex; e, ectopia in region of the ventral striatum and central nucleus of the amygdala; GP, globus pallidus; LGE, lateral ganglionic eminence; MGE, medial ganglionic eminence; MZ, mantle zone; Str, Striatum; SVZ, subventricular zone; VPd, ventral pallidum; VZ, ventricular zone. Scale bars equal 500 μm (A and D) and 300 μm (G).

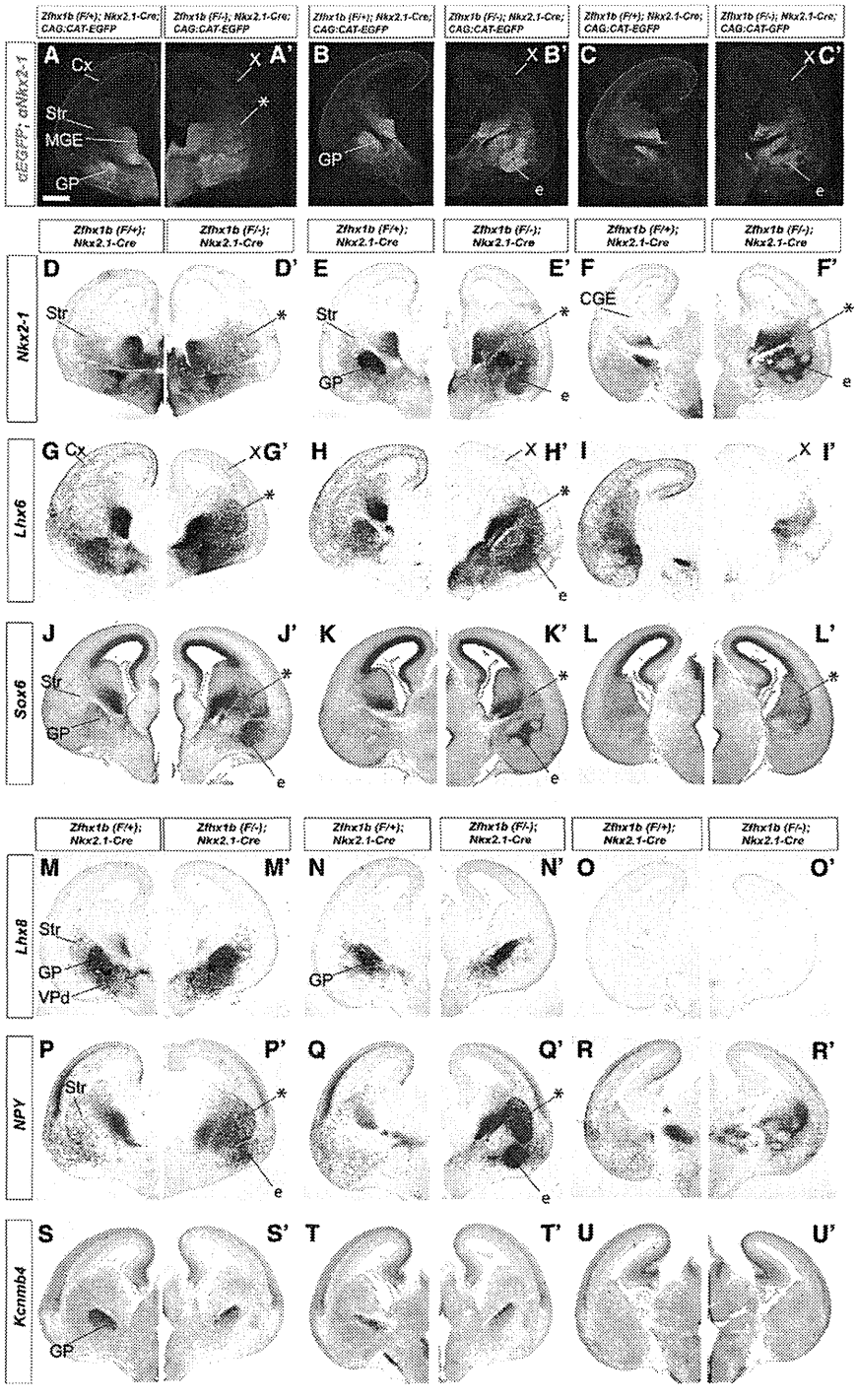

Figure 2. *Zfhx1b* Expression in the MGE Is Required for Interneuron Migration at E15.5

Coronal hemisections of the telencephalon comparing gene expression in three rostral-to-caudal planes of section in control (left side) and *Zfhx1b;Nkx2.1-Cre* conditional mutants (right side).

(A–C′) Two color immunofluoresence detection of EGFP (green) and NKX2-1 (red).

(D–U′) In situ hybridization analysis. *Nkx2-1* (D–F′), *Lhx6* (G–I′), *Sox6* (J–L′), *Lhx8* (M–O′), *NPY* (P–R′), *Kcnmb4* (S–U′). Asterisks show increased numbers of labeled cells in the striatum. X shows reduced number of labeled cells in cortex.

Abbreviations: CGE, caudal ganglionic eminence; Cx, cortex; e, ectopia in region of the ventral striatum and central nucleus of the amygdala; GP, globus pallidus; LGE, lateral ganglionic eminence; MGE, medial ganglionic eminence; MZ, mantle zone; Str, striatum; SVZ, subventricular zone; VPd, ventral pallidum; VZ, ventricular zone. Scale bar equals 500 μm (A).

and S2D–S2F′) and a region contiguous with the caudoventral striatum, which we believe corresponds to the anlage of the central nucleus of the amygdala (labeled e, for ectopia, Figures 2E′′, 2H′, and S2D′; note that Figure S2T shows *Dlx5* expression labeling the central nucleus of the amygdala, CeA). The ectopia in these regions also contained increased expression of *Nkx2-1* and *Sox6* (Figures 2D–2F′ and 2J–2L′). These genes are normally expressed in the subpallial projection neurons such as the globus pallidus, striatal interneurons, and cortical interneurons (*Sox6* only) (Azim et al., 2009; Batista-Brito et al., 2008).

Next, we tested whether the mutant cells that failed to migrate to the pallium had features of the globus pallidus or striatal interneurons. We examined expression of several globus pallidus markers including *Kcnmb4*, *Kctd12*, *Gbx2*, and *Lhx8*. Unlike the abnormal expression of *Lhx6*, *Sst*, *Nkx2-1*, and *Sox6*, expression of *Kcnmb4*, *Kctd12*, *Gbx2*, and *Lhx8* appeared normal in the *Zfhx1b* mutants (Figures 2M–2O′, 2S–2U′, and S2J–S2O′), providing evidence that the abnormal collections of cells correspond either to abnormally migrated cortical interneurons or to striatal interneurons, and not globus pallidus neurons. Furthermore, as *Gbx2* and *Lhx8* expression and function are linked to the development of striatal cholinergic interneurons (Chen et al., 2010; Zhao et al., 2003), these results provided evidence that increased striatal *Nkx2-1* expression did not correspond to cells destined to become striatal cholinergic interneurons.

To distinguish whether the abnormal collections of cells in the mutant striatum were cortical or striatal interneurons, we examined expression of *Cxcr7* and *NPY*. At E15.5, *Cxcr7* marked migrating cortical interneurons and few cells in the striatum (Figures 7J, 7K, and 7L), suggesting that it is a relatively specific cortical interneuron marker (Wang et al., 2011). In the mutant, there was a robust reduction of *Cxcr7* expression in the pattern of migrating cortical interneurons, without a substantive increase

in striatal expression (Figures 7J′, 7K′,and 7L′); a similar result was seen for *Cux2* (not shown). On the other hand, at E15.5, *NPY* expression strongly marks scattered striatal cells (probably interneurons), and relatively few migrating cortical interneurons (note, most of the cortical expression at this age resembles that of immature projection neurons in the cortical plate). In the mutant, there was a robust increase in *NPY* expression in the striatum (Figures 2P–2R′), in a pattern closely resembling the pattern of ectopic *Nkx2-1*, *Lhx6* and *Sox6* (Figures 2D–2L′). Thus, we propose that the mutant cortical interneurons are transformed toward GABAergic striatal interneurons.

Deleting *Zfhx1b* in SVZ of the MGE using *Dlx12b-Cre* Phenocopies Loss of *Zfhx1b* Function in the VZ (*Nkx2.1-Cre*)

Toward defining the stage of differentiation when *Zfhx1b* is required for programming interneurons to migrate to the cortex, and not the striatum, we used the *Dlx12b-Cre* allele (Potter et al., 2008). *Dlx1/2b-Cre* expression begins in subpallial SVZ cells that express the mitotic marker Ki67 (Figures S1T–S1T″), suggesting that Cre recombination occurs in secondary progenitor cells that are mitotically active. Thus, *Dlx12b-Cre* induces recombination beginning in the SVZ of the entire subpallium, whereas *Nkx2.1-Cre* induces recombination in the VZ of the MGE and preoptic area (Figures 1D–1F′).

We analyzed the effect of deleting *Zfhx1b* using *Dlx12b-Cre* at E12.5 and E15.5. In general, all of the phenotypes of MGE-derived cells observed with the *Nkx2.1-Cre* were recapitulated with the *Dlx12b-Cre* (Figures 3, S1, S3), including the strong reduction of tangential migration to the cortex, indicated by analysis of Cre-dependent reporter EGFP expression, and *Lhx6*, *Sst*, and *CXCR7* expression. Like *Nkx2.1-Cre* mutants, *Dlx1/2b-Cre* mutants showed increased numbers of striatal cells that expressed *Lhx6*, *Nkx2-1*, *NPY*, *Sst*, and *Sox6* (Figures 3A–3I′, 3M–3O′, and S3J–S3L′). Furthermore, these mutants did not show an increase in the number of cells that expressed markers of the globus pallius (*Lhx8, Gbx2, Kcnmb4*) or striatal cholinergic interneurons (*Lhx8*, *Gbx2*) (Figures 3J–3L′, 3P–3R′, and S1Q′–S1S′, and data not shown).

Postnatal Analysis of Cortical and Striatal Interneuron Phenotypes in *Nkx2.1-Cre;Zfhx1b* Mutants

Nkx2.1-Cre conditional mutants died between P17 and P21; at P15, mutants weighed ~30% less than their control littermates, a phenotype that was exacerbated by litter size. We did not observe seizures or other neurological/behavioral phenotypes.

We analyzed postnatal day 0 (P0) and P15 *Nkx2.1-Cre;Zfhx1b*$^{F/-}$ conditional mutants to better understand the nature and extent of their cortical and striatal interneuron defects. In the P0 neocortex there was an ~90% reduction in the number of EGFP$^+$ Cre-reporter marked cells, as well as a decrease in Calbindin (CB), *Sst*, and *Lhx6* expressing interneurons (Figures 4A–4C′ and 4S). Likewise, at P15 there was a >90% reduction in number of neocortical EGFP$^+$ cells (Figures 4D–4F′ and 4S). Next, we counted the number cortical interneurons in the *Nkx2-1-Cre* lineage that expressed Parvalbumin (PV) or Sst, which are the two main MGE-derived subtypes (Rudy et al., 2011). We saw a strong reduction in double labeled neurons, with the numbers of EGFP$^+$ interneurons expressing Sst or PV reduced by >90% or more (Figure 4S). The expression of cortical Calretinin (CR), which predominantly marks CGE-derived cortical interneurons, showed little to no change in the *Zfhx1b; Nkx2.1-Cre* conditional mutant (Figures 4F and 4F′).

In the striatum at P0, as we saw at E15.5, there was an increase in the number of cells expressing EGFP (Cre reporter), Sst, and Lhx6 (Figures 4G–4I′); consistent with the hypothesis that *Zfhx1b* mutant cells that were destined to go to the neocortex, instead migrated to the striatum. Additionally, there was a clear increase in the number of striatal cells expressing *nNos*, *NPY*, and *Nkx2-1* (Figures 4J–4K′, S4B, and S4B′), while we observed no change in *Lhx8*, a marker for striatal cholinergic interneurons (Figures S4A and S4A′).

As *NPY*, *Sst*, and *nNos* are also expressed in subsets of cortical interneurons, their increased striatal expression does not provide unequivocal information about whether supernumerary cells correspond to cortical interneurons that failed to correctly migrate, or to interneurons that changed fate due to the mutation. To this end, we searched for a marker that is expressed in striatal, but not cortical interneurons. Substance P receptor (*TacR1)* is robustly expressed in striatal interneurons (Ardelt et al., 1996). We found that *TacR1* is almost exclusively expressed in striatal and not cortical interneurons at E15.5, P0, and P15 (Figures 4L and 4L′, and 4Q and 4Q′, and S4D–S4F′, and data not shown). In *Zfhx1b-Nkx2.1-Cre* mutants at P0, there was increased striatal *TacR1* expression (Figures 4Q and 4Q′), supporting the idea that at least some of the mutant cells are adopting a striatal interneuron identity.

At P15 the number of mutant cells (EGFP$^+$) was roughly the same as in controls, and they were evenly dispersed within the striatum, lacking the cell clusters and ectopia (striatal and caudal amygdala) that were apparent at younger ages (Figures 4M, 4M′, and 4T). The elimination of the excess mutant striatal cells appears to occur through apoptosis, which is robust at P0 (expression of activated cleaved-caspase 6), particularly in the ectopia (Figures S4C–S4C′).

Despite the cell death, *Zfhx1b* conditional mutants at P15 continued to have significantly increased numbers of striatal nNOS, *NPY*, Sst, and *TacR1* expressing cells (183%, 230%, 225%, and 164%; Figures 4N–4Q′ and 4T). Importantly, total striatal PV$^+$ cells were decreased by 58% (Figure 4S). Furthermore, there was no detectable change in *TrkA* expression (Figures 4R, 4R′, and 4T), which marks striatal cholinergic interneurons. We saw very few CR$^+$ cells in the control striatum (1–3 cells per section), which did not noticeably change in the Zfhx1b conditional mutant (data not shown). Thus, *Nkx2.1-Cre;Zfhx1b* mutants have a selective increase in striatal interneurons expressing nNos, *NPY*, Sst, and *TacR1* but have reduced PV interneurons, and no change in cholinergic or CR interneurons.

We also analyzed the gross morphological properties of nNos/*NPY*/Sst striatal interneurons in the Zfhx1b mutant and found that, like control brains, *Zfhx1b* conditional mutants had Sst processes restricted to the matrisomes (Chesselet and Graybiel, 1986), in a lateral to medial gradient (Figures S4G–S4I′, arrowheads mark CB-poor striosomes), suggesting that the overproduced nNos/*NPY*/Sst interneurons in the Zfhx1b conditional

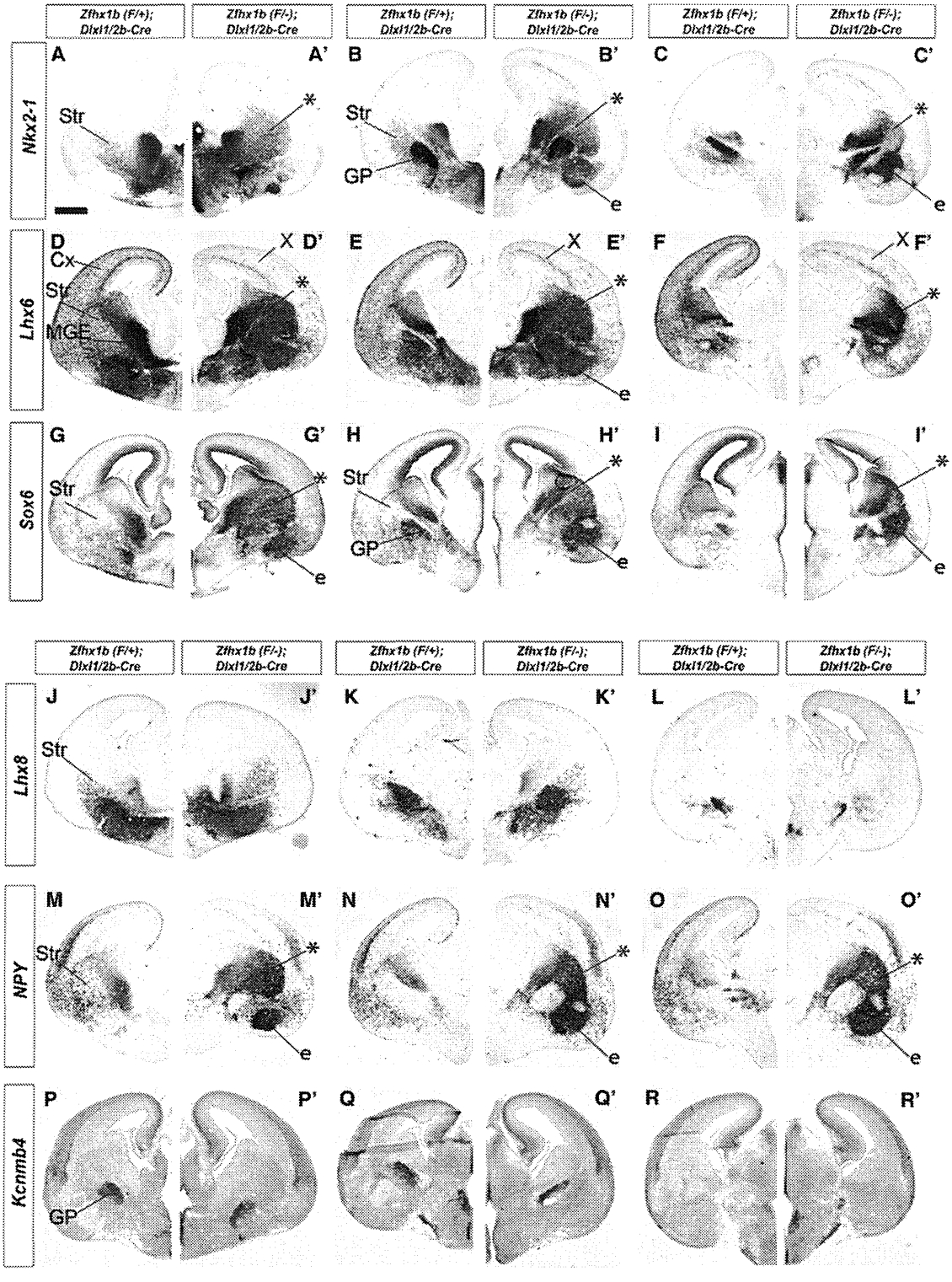

Figure 3. *Zfhx1b* Expression in the SVZ of the MGE Is Required for Interneuron Migration at E15.5

Coronal hemisections of the telencephalon comparing gene expression in three rostral-to-caudal planes of section in control (left side) and *Zfhx1b Dlxl12b-Cre* conditional mutants (right side). In situ hybridization analysis of *Nkx2-1* (A–C′), *Lhx6* (D–F′), *Sox6* (G–I′), *Lhx8* (P–R′), *NPY* (M–O′), *Kcnmb4* (P–R′). Asterisks show increased numbers of labeled cells in the striatum. X shows reduced number of *Lhx6*$^{+}$ cells in cortex. Abbreviations: CGE, caudal ganglionic eminence; Cx, cortex; e, ectopia in region of the ventral striatum and central nucleus of the amygdala; GP, globus pallidus; LGE, lateral ganglionic eminence; MGE, medial ganglionic eminence; MZ, mantle zone; Str, striatum; SVZ, subventricular zone; VPd, ventral pallidum; VZ, ventricular zone. Scale bar equals 500 μm (A).

mutant share grossly similar morphological properties with wild-type striatal interneurons.

Zfhx1b Expression Is Downstream of *Dlx1/2* in the Developing Basal Ganglia

Dlx1 and *Dlx2* are necessary for subpallial development, including interneuron migration to the cortex (Anderson et al., 1997a; Long et al., 2009a; Long et al., 2009b; Yun et al., 2002a); thus, we examined *Zfhx1b* RNA expression in *Dlx1/2* constitutive null mutants using in situ hybridization (Figures 5A–5B′). In control brains at E12.5 and E15.5, *Zfhx1b* was expressed in the VZ and SVZ of the subpallium, in addition to its previous described expression in the cortical plate and SVZ (Miquelajauregui et al., 2007; Seuntjens et al., 2009). *Zfhx1b* expression in the subpallial MZ was restricted to dispersed cells in the LGE and to a nucleus forming near the ventral medial ganglionic eminence (MGE) (Figures 1A, 5A, and 5B). In *Dlx1/2*$^{-/-}$ mutants, *Zfhx1b* expression was strongly and specifically decreased in the SVZ of the entire subpallium; expression in the subpallial VZ was maintained, albeit perhaps reduced (Figures 5A–5B′).

Toward defining the mechanisms that regulate *Zfhx1b* expression in the developing subpallium, we identified two regulatory elements near the *Zfhx1b* locus that drive expression in the developing subpallium. These enhancers, here named #649 and #675, were identified by virtue of their extremely strong evolutionary conservation (Figures 5C–5G) and their reproducible enhancer activity in the forebrain of mouse embryos in transgenic experiments (Figures 5H–5I; Visel et al., 2007, 2008). The other genes in this region do not have known expression in the developing subpallium. Analysis of enhancer activity at E11.5 in transgenic whole mounts and sections showed that both enhancers drive LacZ expression in the subpallium, including the SVZ of the MGE (Figures 5H and 5I). The spatial overlap of enhancer activities and *Zfhx1b* mRNA expression suggests that these two elements are distant-acting transcriptional activators of *Zfhx1b* in the developing subpallium. Computational analysis identified multiple candidate homeobox binding sites (asterisks in Figures 5D and 5E and highlighted regions in 5F and 5G).

To test whether Dlx2 can regulate these candidate *Zfhx1b* enhancers we used a luciferase reporter assay. Co-transfection of a luciferase reporter construct containing enhancers #649 and #675 with a *Dlx2* expression vector in P19 cells showed that DLX2 strongly activates luciferase transcription when these elements are present (Figure 5J).

To determine whether DLX2 directly regulates enhancers 649 or 675, we performed chromatin immunoprecipitation (ChIP)-qPCR of E13.5 basal ganglia using a DLX2 antibody. We found enrichment over several homeodomain-containing regions of enhancers 649 and 675, with a particular domain of #675 (region #3) showing the strongest enrichment as compared to control regions of the genome (Figure 5K). Also, the relative enrichment of the enhancer fragments was eliminated when a DLX2 polypeptide was included in the immunoreaction as a negative control (Figure 5K).

In summary, we have identified two candidate distant-acting gene regulatory elements whose activity patterns suggest that they contribute to *Zfhx1b* expression in the developing subpallium. These enhancer elements are activated by DLX2 in luciferase reporter assays and are bound by DLX2 in vivo, providing strong evidence that subpallial *Zfhx1b* expression directly depends on *Dlx1/2*. Consistent with this, we observed marked alterations of *Zfhx1b* expression in the subpallial SVZ of *Dlx1/2*-deficient mice. Taken together, these results raise the possibility that the loss of *Zfhx1b* expression in the SVZ could contribute to the defects in differentiation and interneuron migration seen in *Dlx1/2* mutants. To investigate this possibility, we compared the phenotypes of the conditional *Zfhx1b* and *Dlx1/2*$^{-/-}$ mutants.

Dlx1/2$^{-/-}$ Constitutive and *Zfhx1b* Conditional Mutants Have Similar Changes in Gene Expression Related to Their Defects in Interneuron Migration

As *Zfhx1b* expression in the subpallial SVZ was greatly reduced in the *Dlx1/2* mutants (Figures 5A–5B′), and because interneuron migration to the cortex was greatly reduced in both the *Dlx1/2*$^{-/-}$ and *Zfhx1b* mutants, we hypothesized that loss of *Zfhx1b* may underlie some of the interneuron migration phenotype of the *Dlx1/2*$^{-/-}$ mutants. To evaluate this idea, we compared gene expression phenotypes of the *Dlx1/2*$^{-/-}$ constitutive null mutant with the *Zfhx1b* conditional (*Nkx2.1-Cre*) mutant at E15.5 (Figure 6).

Indeed, changes in *Nkx2-1* and *Sox6* expression were similar in the *Dlx1/2*$^{-/-}$ and *Zfhx1b* mutants. *Nkx2-1* and *Sox6* RNAs are normally expressed in similar patterns at E15.5 (Figures 6A, 6B, 6C, 6G, 6H, and 6I); in wild-type brains, both RNAs are maintained in the MGE, and in putative striatal interneurons and globus pallidus neurons, while they are downregulated in the MGE-derived cortical interneuron lineage (*Nkx2-1*-, *Sox6*^{low}). Both *Dlx1/2*$^{-/-}$ and *Zfhx1b* mutants show increased numbers of *Nkx2-1*$^{+}$ and *Sox6*$^{+}$ cells in the striatum/LGE (asterisks in Figure 6; note: the *Dlx1/2*$^{-/-}$ mutant striatum is small due to *Dlx*-function in the LGE) (Anderson et al., 1997b; Yun et al., 2002a).

Lhx6^{+} cells are lacking throughout the cortex and increased in the striatum of both the *Dlx1/2*$^{-/-}$ and *Zfhx1b* mutants (Figures 6D–6F″). Likewise, *Sst*$^{+}$ and *NPY*$^{+}$ cortical interneurons were lost, whereas their expression was increased in the striatum (Figures 6J–6L″; *Sst* data not shown).

RNA Expression Array Analysis Identifies Candidate Mediators of *Zfhx1b* Function

Toward identifying the molecular mechanisms underlying the *Zfhx1b* mutant phenotype we used an RNA expression microarray analysis. We compared gene expression from the E12.5 MGE of *Nkx2.1-Cre; Zfhx1b*$^{F/-}$ mutants to that of *Nkx2.1-Cre; Zfhx1b*$^{F/+}$ control littermates. Table S1 (see Table S3 for an extended version) lists the most highly upregulated and downregulated genes. Overall, a larger number of genes were found to be significantly upregulated than downregulated in *Zfhx1b* mutants, which may reflect *Zfhx1b*'s function as a recruiter of repressive transcriptional complexes (van Grunsven et al., 2003; Verschueren et al., 1999; Verstappen et al., 2008). We verified the results for many of the genes by performing in situ RNA hybridization on E12.5 control and mutant brains (Figure S6 and data not shown).

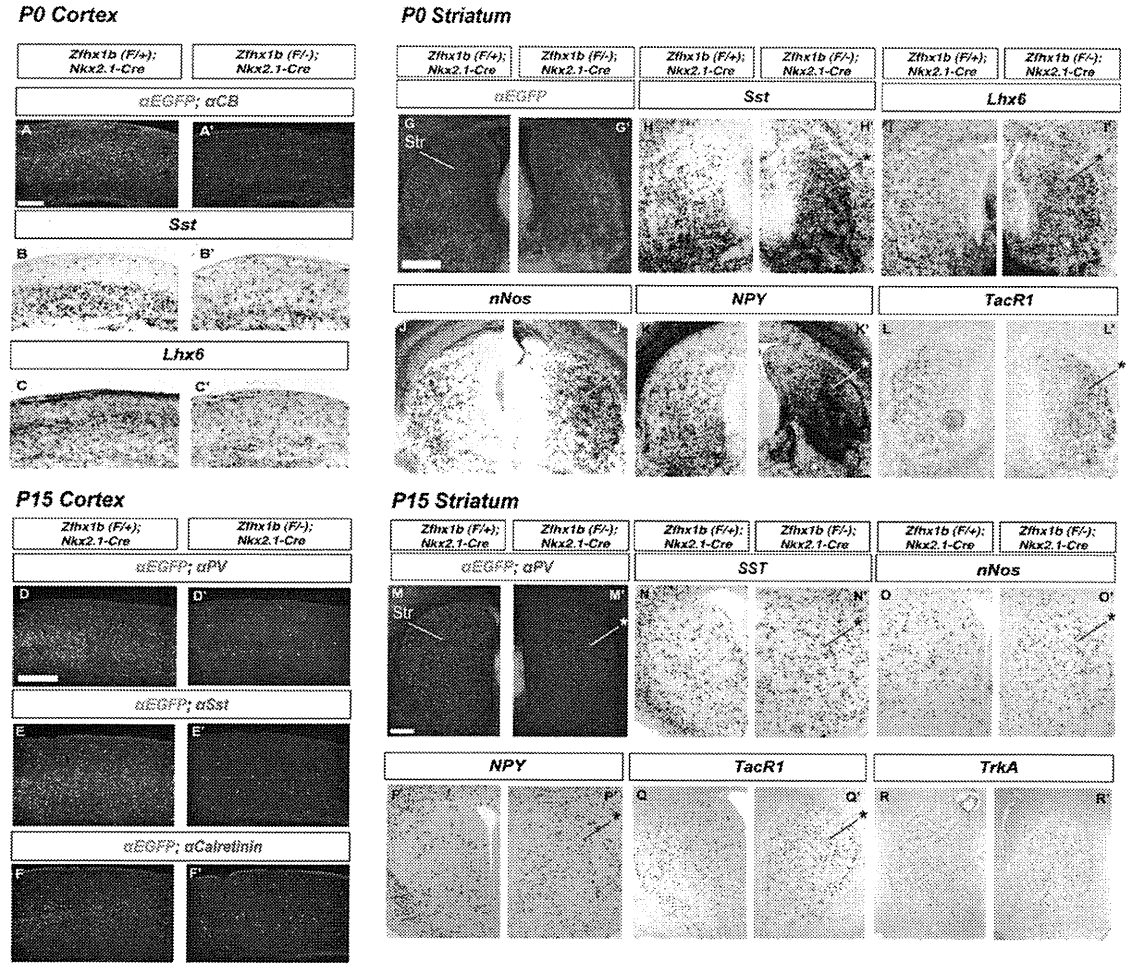

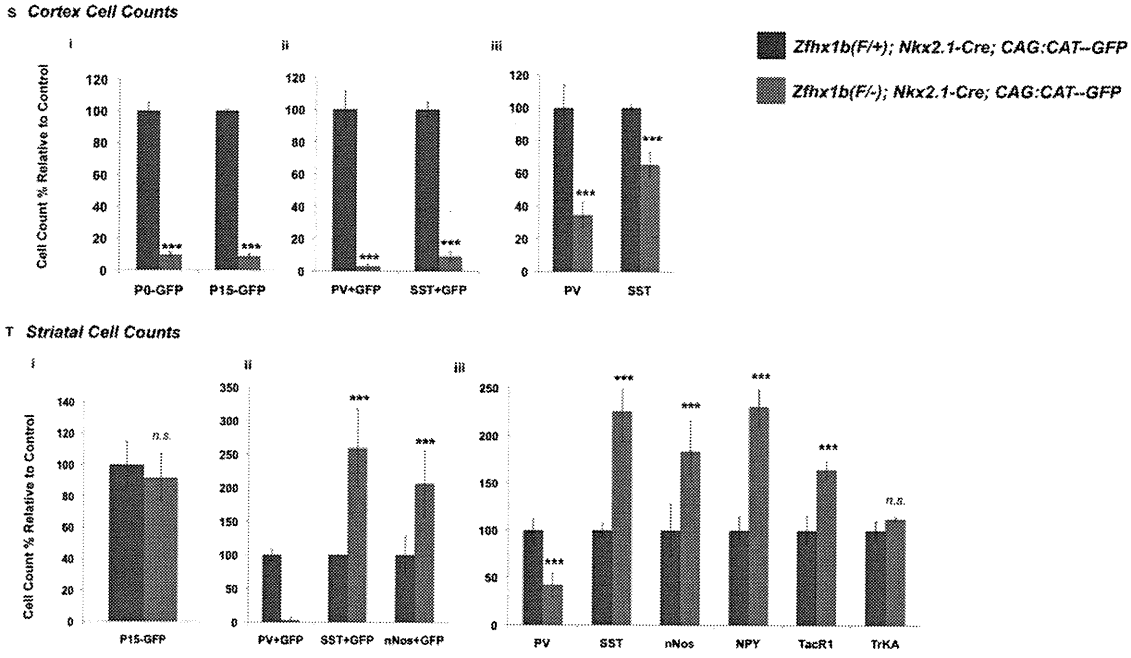

(legend continued on next page)

We were most interested in genes that were altered in both the *Nkx2.1-Cre* and *Dlx12b-Cre Zfhx1b* mutants, given that both mutants showed altered interneuron migration and specification. Six genes fell into this category: *cMaf*, *MafB*, *CXCR7*, *Dlk1*, *Cited1*, and *Gpc4* (Figures 7 and S6). *Dlk1*, *Cited1*, and *Gpc4* were upregulated in the MGE both mutants (Figure S6). *cMaf*, *MafB*, and *CXCR7* were downregulated in the MGE and migrating interneurons; later in the paper, we focused more on these genes (Figures 7 and S6); below, we discuss the other genes.

Dlk1 expression was strongly increased in the VZ and SVZ of the MGE in the *Nkx2.1-Cre* mutant and increased weakly only in the SVZ of the MGE in the *Dlx12b-Cre* mutant. (Figures S6J–S6L′ and S6HH-S6JJ″). Given that *Zfhx1b*'s function was required in the SVZ of the MGE, the increase in *Dlk1* expression could play a role in the phenotype. *Dlk1* encodes a secreted delta-like ligand (Ferrón et al., 2011; Moon et al., 2002) that could alter Notch signaling. We used electroporation to increase *Dlk1* expression in wild-type MGE, but failed to identify a change in interneuron migration (data not shown).

Other genes related to Notch-signaling were also identified in the array analysis, including the *Id2* and *Id4* helix-loop-helix and *Sox6* HMG-box transcription factors (Table S1). Expression of *Id4* was increased in the VZ of the *Nkx2.1-Cre* mutant; however, no change in expression was detected in the *Dlx12b-Cre* mutant (Figures S6M–S6O′ and S6KK–S6MM′); this implies that *Id4* does not contribute to the interneuron phenotype. *Id2* expression showed a subtle expression increase in the *Nkx2.1-Cre* mutant (not shown); like *Id4*, we did not find a change in its expression in the *Dlx1/2b-Cre* mutant (not shown). *Sox6* expression was also increased based on the array and an increase was seen in both *Nkx2.1-Cre* and *Dlx1/2b-Cre* mutants by in situ hybridization at E12.5 (Table S1, Figures S1F–S1F′, and data not shown), which became more pronounced at E13.5 and E15.5 (Figures 2J–2L′ and 3G–3I′). Of note, *Sox6* represses MGE expression of *Ascl1* (*Mash1*) (Azim et al., 2009), a basic-helix-loop-helix transcription factor whose expression is promoted by Notch-signaling.

Expression of *Cited1*, a p300-binding transcriptional co-activator that promotes signaling in the TGF-beta pathway (Gerstner and Landry, 2007) was increased in the SVZ of the ventral MGE and POA in both the *Nkx2.1-Cre* and *Dlx12b-Cre* mutants (Figures S5S–S5U′ and S5QQ–S5SS′). This is of interest given that ZFHX1B acts as a SMAD-binding transcriptional corepressor (Vandewalle et al., 2009). Thus, *Cited1* and *Zfhx1b* may function antagonistically in MGE development. *Gpc4* expression in the SVZ of the MGE was increased in both mutants (Figures S5V–S5X′ and S5TT–S5WW′). Glypicans (GPC) are extracellular matrix proteins that promote FGF-signaling (Jen et al., 2009).

Expression of genes related to oligodendrogenesis, including *Olg1* and *GPR17* (Chen et al., 2009; Lu et al., 2000) were downregulated on the array in the *Nkx2.1-Cre* mutant (Table S1); we failed to detect *GPR17* expression by in situ hybridization and *Olg1* expression was weak. For this reason, we studied *Olg2* expression; its expression was reduced in the SVZ of the MGE at E12.5 (Figures S5P–S5R′). The downregulation of oligodendrocyte markers may be related to the increase in *ID4* RNA; ID proteins can repress oligodendrogenesis (Wang et al., 2001). By E15.5, we did not detect a change in *Olg2* expression (Figures S2P–S2R′). The *Dlx12b-Cre* mutant did not show changes in *Olg2* expression (Figures S5NN–S5PP′), suggesting the *Zfhx1b* function in the VZ, and not SVZ, regulates oligodendrogenesis.

Zfhx1b Is Required for Expression of Genetic Markers of Cortical Interneurons: *cMaf*, *MafB*, and *Cxcr7*

The gene expression array showed a ~3-fold reduction in the expression of *cMaf* (*v-Maf*), a leucine zipper-containing transcription factor (Table S1). *cMaf*, and its relative *MafB*, have been reported to be expressed in cortical interneurons (Cobos et al., 2006; Faux et al., 2009; Zhao et al., 2008). Likewise, the array identified reduced expression of *CXCR7*, whose expression and function are required during cortical interneuron migration (Sánchez-Alcañiz et al., 2011; Wang et al., 2011).

We compared *cMaf*, *MafB*, and *Cxcr7* RNA expression at E12.5 and E15.5 and identified some important features (Figures 7, S2A–S2C, and S6D–S6F). *cMaf*, *MafB*, and *Cxcr7* RNAs were expressed in the SVZ of the dorsal MGE (and not the ventral MGE) and were maintained in cells migrating through the LGE and CGE and then into the cortex at E12.5 and E15.5 (Figure 7, S2A–S2C, and S6D–S6F). *cMaf*, *MafB*, and *CXCR7* appear to be excellent markers of the cortical interneuron lineage, as we did not detect their expression in other MGE-derived structures, such as the ventral pallidum or globus pallidus at E12.5, E15.5, or P0 (Figures 7, S2A–S2C, S6D–S6F, and data not shown). In the E15.5 and P0 striatum, these genes showed little expression (Figure 7), except for *MafB* and *cMaf* in a very small population of cells (data not shown). Thus, unlike other cortical interneuron markers that are also expressed in striatal interneurons (e.g., *Dlx1*, *Lhx6*, *Parvalbumin*, *Sst*), *cMaf*, *MafB*, and *CXCR7* expression largely mark only cortical interneurons.

We then compared *cMaf*, *MafB*, and *Cxcr7* expression in E12.5 and E15.5 control (*Zfhx1b* heterozygotes), *Zfhx1b* conditional mutants (*Nkx2.1-Cre* and *Dlx12b-Cre*) and the *Dlx1/2*$^{-/-}$

Figure 4. *Zfhx1b* Expression in the MGE Regulates the Numbers and Fate of Postnatal (P0 and P15) Cortical and Striatal Interneurons

Coronal hemisections showing the neocortex (A–F) and the striatum (G–R), comparing gene expression in control (left side) and *Zfhx1b;Nkx2.1-Cre* conditional mutants (right side).

(A and A′, D–F′, G and G′, and M and M′) Two color immunofluorescence with anti-EGFP (Cre reporter; green) and interneuron markers (red); other panels show in situ hybridization results.

(S) Cell counts, control relative to mutant, of: total Cre-reporter EGFP$^+$ cell numbers in the P0 and P15 cortex (left); of the number of cells that had colocalization of the EGFP Cre-reporter with Sst or PV at P15 (middle); of the total levels of Sst and PV in the P15 cortex (right).

(T) Cell counts, control relative to mutant, of EGFP$^+$ Cre-reporter cells in the P15 striatum (left); of EGFP-colocalization with PV, Sst, and nNos in the P15 striatum (middle); and of the total numbers of the markers PV, Sst, nNos, NPY, TacR1, and TrkA in the P15 striatum (right).

Error bars represent standard deviation. Scale bar equals 500 μm (A, D, G, and M). *$p < 0.05$; **$p < 0.01$.

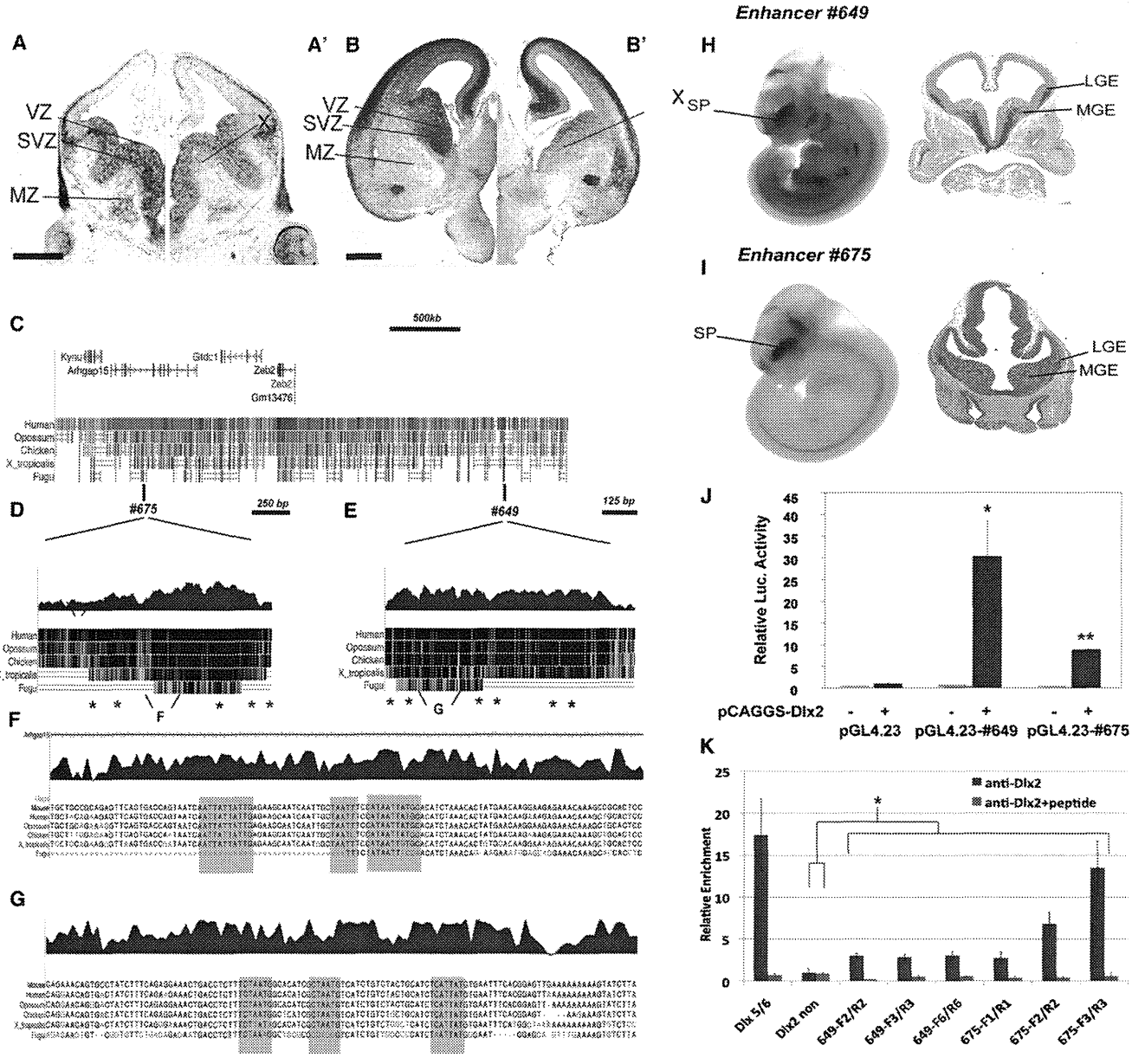

Figure 5. *Dlx1&2* Are Required for *Zfhx1b* Expression in the SVZ of the Subpallium

(A–B′) Coronal hemisections of the telencephalon comparing *Zfhx1b* expression in *Dlx1*$^{+/-}$ and *Dlx1/2*$^{-/-}$ at E12.5 (A and A′) and E15.5 (B and B′). Note the greatly reduced *Zfhx1b* expression in the SVZ of the LGE and MGE. X denotes reduction in *Zfhx1b* expression in the SVZ.

(C–K) Regulatory elements near *Zfhx1b* that drive subpallial expression are bound by DLX2 in vivo and are positively regulated by DLX2. (C) Relative genomic position of two ultraconserved DNA elements near the Human *Zfhx1b* (*Zeb2*) locus, #675 (D) and #649 (E) (data from http://genome.ucsc.edu/). (D and E) Genomic alignment of enhancers #675 and #649; each contain a number of conserved consensus homeobox sites (asterisks). (F and G) Base-resolution view of regions with homeobox sites within #649 and #675, which are heavily conserved across vertebrate species and are similar to known DLX2 binding sites (Potter et al., 2008). (H and I) Whole-mount E11.5 *enhancer-lacZ* transgenic mouse embryos that demonstrated *lacZ* expression (X-Gal staining) in the ganglionic eminences (subpallium) (H′ and I′). (J) Luciferase assay demonstrating DLX2-dependent transcriptional activation (*pCAGGS* vector) mediated by enhancers #649 and #675 upstream of luciferase (*pGL4.23* vector). (K) Blue bars: DLX2 ChIP qPCR assay (n = 3) demonstrates anti-DLX2 binding to chromatin from E13.5 ganglionic eminences to subdomains of enhancers #675 and #649 and the positive control (Dlx5/6 enhancer), and not to the negative control region (a nonconserved domain upstream of *Dlx2*). Red bars: addition of a DLX2 peptide blocks the anti-DLX2 binding.

Abbreviations: Cx, cortex; LGE, lateral ganglionic eminence; Luc, luciferase; MGE, medial ganglionic eminence; MZ, mantle zone; SP, subpallium; SVZ, subventricular zone; VZ, ventricular zone. Error bars represent standard deviation. Scale bar equals 500 μm (A and B). ***p < .001; n.s., not significant.

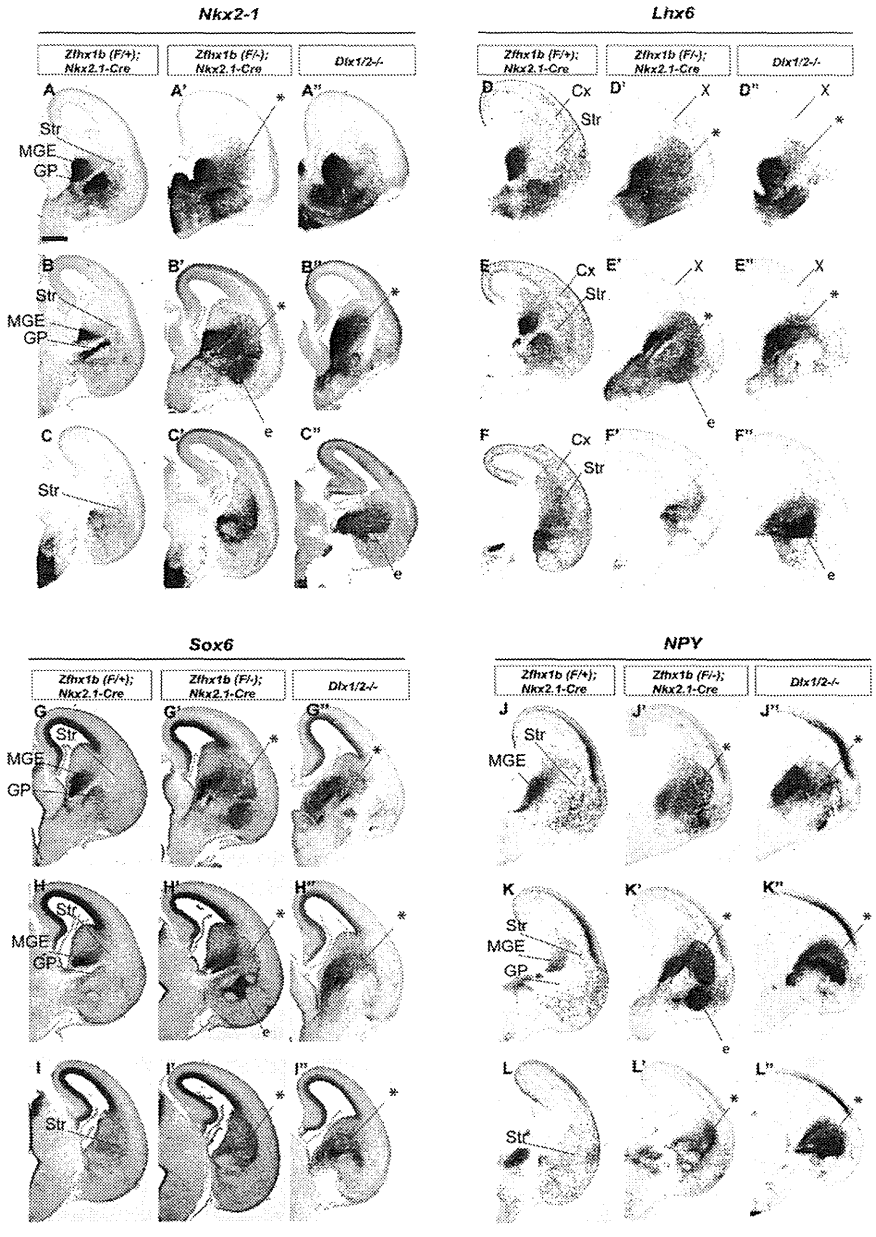

Figure 6. *Zfhx1b;Nkx2.1-Cre* and *Dlx1/2*$^{-/-}$ Mutants Both Fail to Repress *Nkx2-1* and *Sox6*, Lose Cortical Interneurons, and Accumulate MGE Cells in Their Striatum

Coronal hemisections of the E15.5 telencephalon comparing gene expression in three rostral-to-caudal planes of section in controls (left side) and mutants (right side). In situ hybridization analysis of *Nkx2-1* (A–C″), *Lhx6* (D–F″), *Sox6* (G–I″), and *NPY* (J–L″) expression was assessed for control, *Zfhx1b;Nkx2.1-Cre* mutants, and *Dlx1/2*$^{-/-}$ mutants. Asterisks show increased numbers of labeled cells in the striatum. X shows reduced number of *Lhx6*$^{+}$ cells in cortex. Abbreviations: CGE, caudal ganglionic eminence; Cx, cortex; e, ectopia in region of the ventral striatum and central nucleus of the amygdala; GP, globus pallidus; LGE, lateral ganglionic eminence; MGE, medial ganglionic eminence; MZ, mantle zone; Str, striatum; SVZ, subventricular zone; VPd, ventral pallidum; VZ, ventricular zone. Scale bar equals 500 μm (A).

constitutive mutant (Figures 7, S2A–S2C″, and S3A–S3I′). *cMaf* expression was nearly eliminated in all three mutants. Much of the remaining *cMaf* expression was in scattered blood cells and in the choroid plexus (Figures 7H′ and 7H″). *MafB* and *Cxcr7* were also greatly reduced in the SVZ of the ganglionic eminences, although they were not as strongly downregulated as *cMaf* (Figures 7, S2A–S2C′, S3D–S3I′, S6D–S6I′, and S6BB–S6GG′). Therefore, *Zfhx1b* (and *Dlx1&2*) were required for *cMaf*, *MafB*, and *Cxcr7* expression, which are highly specific markers of immature migrating cortical interneurons (*cMaf* and *MafB* are specific for MGE-derived interneurons). Thus, the loss of *cMaf*, *MafB*, and *Cxcr7* expression in *Zfhx1b* conditional mutants (*Nkx2.1-Cre* and *Dlxl12b-Cre*) provides additional evidence that cortical interneurons fail to be specified.

Next, we determined at a cellular resolution when *cMaf* expression begins in developing cortical interneurons (Figures 7M–7M‴). Given that *cMaf* expression in the dorsal MGE and migrating cortical interneurons is dependent on *Zfhx1b* expression, and that repression of *Nkx2-1* in these regions is also *Zfhx1b* dependent, we analyzed whether or not *cMaf* and *Nkx2-1* are coexpressed in these cells. To this end, we performed a triple-labeling analysis: fluorescent in situ hybridization to detect *cMaf* in combination with immunofluorescence to label NKX2-1 and the EGFP^{+} *Nkx2.1-Cre* lineage (EGFP expression from *CAG-CAT-EGFP*, the Cre reporter allele). We found that *cMaf* RNA was expressed in EGFP^{+} cells derived from the MGE lineage that were migrating through the LGE corridor (LGE-Co) on route to the cortex (Figures 7M′, 7M″, and 7M‴). These cells were NKX2-1^{-}. On the other hand, NKX2-1 was expressed in *cMaf* −cells of the globus pallidus (Figures 7M, 7M″, and 7M‴). Thus, as NKX2-1 expression is repressed in immature cortical interneurons, *cMaf* expression begins.

DISCUSSION

Herein we demonstrate that *Zfhx1b* subpallial expression is directly positively regulated by *Dlx1&2* and is required in the MGE to generate cortical interneurons that express *Cxcr7*, *MafB*, and *cMaf*. In its absence, *Nkx2-1* expression is not repressed, and cells that ordinarily would become cortical interneurons are transformed toward the *NPY/nNos/Sst* subtype

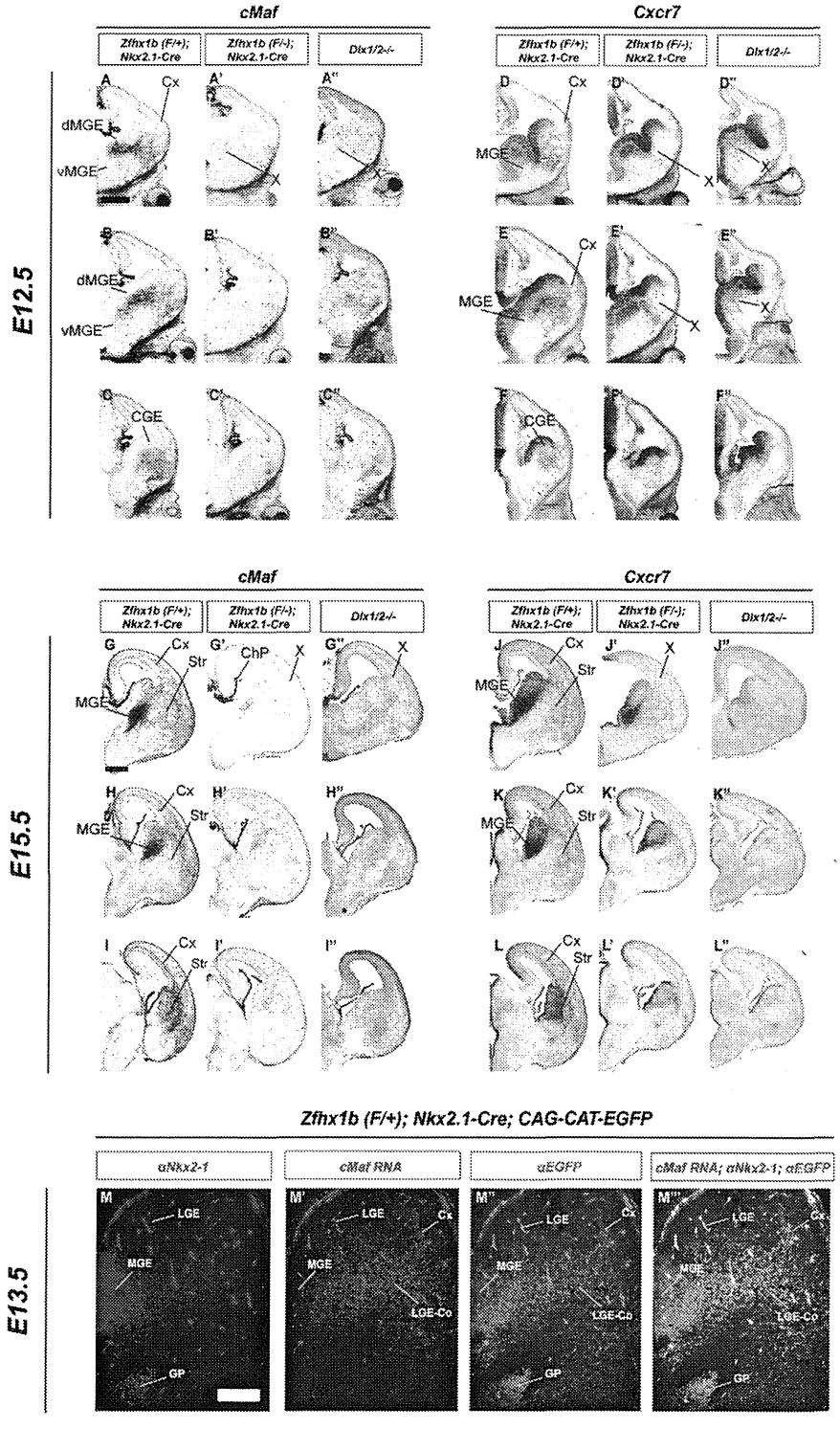

Figure 7. *cMaf* and *CXCR7* Are Highly Specific Markers of the Cortical Interneuron Lineage that Are Lost in *Zfhx1b* Conditional Mutants and *Dlx1/2*$^{-/-}$ Mutants

Coronal hemisections of the E12.5 (A–F″) and E15.5 (G–L″) telencephalon comparing *cMaf* (A–C″; G–I″) and *CXCR7* (D-F″; J-L″) RNA expression by in situ hybridization in three rostral-to-caudal planes of section in control (left panels), *Zfhx1b;Nkx2.1-Cre* conditional mutants (middle panels), and *Dlx1/2*$^{-/-}$ mutants (right panels). X shows reduced/absent *cMaf*$^{+}$ or *CXCR7*$^{+}$ cells in cortex or ganglionic eminences. Abbreviations: CGE, caudal ganglionic eminence; ChP, choroid plexus; Cx, cortex; LGE Co, LGE corridor; dMGE, dorsal medial ganglionic eminence; vMGE, ventral medial ganglionic eminence; Str, striatum. Scale bars are equal to 500 μm (A) and 200 μM (M).

Zfhx1b Regulates MGE Cell-Type Generation

The MGE generates multiple cell types, including GABAergic interneurons of the cortex and striatum, GABAergic projection neurons of the basal ganglia (e.g., GP), cholinergic neurons of the striatum and basal telencephalon and oligodendrocytes (Flandin et al., 2010; Petryniak et al., 2007; Xu et al., 2008). The MGE generates roughly 60% of all GABAergic cortical interneurons; these express *PV*, *Sst*, *NPY*, and *nNos* (Gelman and Marín, 2010; Rudy et al., 2011).

The MGE also generates striatal interneurons. There are three subtypes of GABAergic striatal interneurons: *PV*$^{+}$, *nNos/NPY/Sst*$^{+}$ *and CR*$^{+}$ (Tepper et al., 2010). The striatum also has cholinergic interneurons. The cholinergic population is marked and regulated by *Gbx2*, *Islet1*, and *Lhx8* (Chen et al., 2010; Fragkouli et al., 2009), and the neurotrophin receptor TrkA (Sanchez-Ortiz et al., 2012).

The ventral MGE is not a major source for cortical interneurons based on fate mapping using *Shh-Cre* (Flandin et al., 2010). Thus, the dorsal MGE must be the source of most MGE-derived cortical and striatal GABAergic interneurons. It is poorly understood whether these cell types are generated from distinct subregions, from distinct but intermixed progenitors, or from the same progenitors in a stochastic or temporally modulated program. While the same neuroepithelial progenitor can generate different types of cortical interneurons (PV and Sst) (Brown et al., 2011), it is not known whether cortical and striatal interneurons are derived from the same progenitor.

of striatal GABAergic interneuron. Furthermore, it is possible that the *Zfhx1b*$^{-/-}$ phenotype is also caused by defects in migration and differentiation that contribute to the formation of subpallial ectopia. However, below we largely concentrate on discussing the evidence that *Zfhx1b* regulates cell-type specification.

Zfhx1b was required to generate GABAergic cells that migrate to the cortex, and to repress the generation GABAergic cells that migrate to the striatum. We suggest that *Zfhx1b* promotes a fate switch between cortical interneurons and *nNos/NPY/Sst* striatal interneurons through repression of *Nkx2-1* expression. Furthermore, *Zfhx1b* mutants have reduced striatal *PV* interneurons (Figures 4M and 4M′); thus, *Zfhx1b* could also control this fate decision. *Zfhx1b* is required in the MGE SVZ, and not the VZ, to promote the specification of pallial interneurons, as we observed largely the same phenotype using *Dlxi12b-Cre* (SVZ recombination, Figures 3, S1, and S3) and *Nkx2.1-Cre* (VZ recombination; Figures 1, 2, S1, and S2).

We identified perhaps the first specific early marker of dorsal MGE-derived cortical interneurons: *cMaf* (Figure 7). *cMaf* and *Mafb* expression are dependent on *Zfhx1b* and *Dlx1/2* function (Figures 7, S2A–S2C′, S3D–S3F′, S6D–S6F′, and S6BB–S6DD′; Cobos et al., 2006; Long et al., 2009a; Long et al., 2009b). Notably, neither *cMaf* nor *Mafb* are strongly expressed prenatally in neurons of the striatum (interneurons and medium spiny neurons), suggesting that prenatally they may be specific markers of the cortical interneuron lineage. Currently, *Maf* function in the brain has only been studied in the hindbrain (Cordes and Barsh, 1994).

Zfhx1b Connects the *Nkx2-1* and *Dlx* Transcription Pathways

There is genetic evidence for at least three parallel (although interacting) transcriptional pathways in the MGE that are required for cortical interneuron development: the (1) *Ascl1* (*Mash1*), (2) *Dlx*, and (3) *Nkx2-1* pathways (Long et al., 2009a, 2009b). The *Nkx2-1* pathway is the core mediator of MGE regional and cell identity (Butt et al., 2007; Sussel et al., 1999); it functions through induction of *Lhx6* and *Lhx8* (Sussel et al., 1999). *Lhx6* is essential for induction of *Mafb* and *Shh* in neurons, maintenance of *Sox6* in interneurons, and the differentiation of Sst and Parvalbumin cortical interneurons (*Lhx6*) (Liodis et al., 2007; Zhao et al., 2008); *Lhx8* is required in cholinergic striatal interneurons (*Lhx8*) (Fragkouli et al., 2009).

Only a subset of MGE neuronal derivatives maintain *Nkx2-1* and *Lhx8* expression, such as the globus pallidus and cholinergic striatal interneurons (Marin et al., 2000), whereas MGE-derived cortical interneurons suppress *Nkx2-1* and *Lhx8* expression (Nóbrega-Pereira et al., 2008). We propose that *Dlx* and *Nkx2-1* pathways interact at this step. We demonstrated that *Dlx1/2* were required for *Zfhx1b* expression in the subpallial SVZ (Figure 4) and that *Zfhx1b* was required for repression of *Nkx2-1*, but not of *Lhx8* (Figures 2D–2F′, 2M–2O′, 3A–3C′, and 3J–3L′). Thus, in the absence of *Zfhx1b*, dorsal MGE-derived neurons continued to express *Nkx2-1*, *Sox6*, and *Lhx6*, and migrate into the striatum and not the cortex. These cells failed to express markers of cortical interneurons (*Cxcr7*, *cMaf*, and *MafB*) (Figures 7A–7L″ and S5A–S5I′), but highly expressed the striatal GABAergic subtype markers *NPY*, *nNos*, and *Sst* (Figures 2P–2R′ and 3M–3O′; Tepper et al., 2010). Additionally, there was increased expression of *TacR1*, which is robustly expressed in Sst^+ and $ChAT^+$ striatal interneurons, and in very few cortical interneurons (Ardelt et al., 1996; Figures S4D–S4F′).

Finally, *Zfhx1b* mutants did not exhibit clear phenotypes of striatal cholinergic interneurons or the GP. Thus, we propose a distinct *Zfhx1b*-independent mechanism for the generation of the GP and cholinergic neurons; the latter depends on the maintenance of *Lhx8*, perhaps in combination with *Islet1* and *Gbx2* (Chen et al., 2010; Fragkouli et al., 2009).

Downstream of *Zfhx1b* in the MGE Cells

It is unclear whether *Zfhx1b* has a common molecular mechanism in all developing cells. *Zfhx1b* mediates some of its functions through interactions with SMAD proteins, and thus participates in TGF-beta signaling (Vandewalle et al., 2009). Expression of the SMAD-binding transcriptional coactivator *Cited1* was increased in *Zfhx1b* mutants (Figure S6). The link to SMAD signaling is intriguing because SMAD dominant-negative expression can inhibit interneuron tangential migration (Maira et al., 2010).

In the pallium, *Zfhx1b* functions in both progenitors and neurons. In hippocampal progenitors, it functions upstream of Wnt signaling to control development of the entire region (Miquelajauregui et al., 2007). In neocortical neurons, *Zfhx1b* regulates *neurotrophin-3* and *Fgf9* expression, to control cortical progenitors (Seuntjens et al., 2009). We did not observe similar regulatory changes in the *Zfhx1b* mutant MGE.

While *Zfhx1b* in the MGE SVZ regulates the switch between cortical and striatal interneurons, *Zfhx1b* is also expressed in the VZ of the MGE (Figure 1A). Two genes related to Notch signaling were upregulated in the mutant MGE VZ, including the secreted delta-like ligand *Dlk1* (Ferrón et al., 2011; Moon et al., 2002) and the HLH transcription factor *ID4* (Yun et al., 2004; Figures S6J–S6O′). *Dlk1* upregulation in the VZ and SVZ could alter the balance of cell fate decisions.

Previous studies suggested that *Nkx2-1* promotes interneuron integration into the striatum via repression of Npn2/Sema3-dependent repulsion (Marín et al., 2001; Nóbrega-Pereira et al., 2008). We did not detect a change in *Npn2* and *Npn1* RNA expression in migrating immature *Zfhx1b* mutant interneurons at E12.5. On the other hand, van den Berghe et al. (2012) (this issue of *Neuron*) present evidence that *Zfhx1b* regulates interneuron migration through the Netrin receptor *Unc5b*.

Zfhx1b and Human Disease

Mowat-Wilson syndrome (MWS) is caused by a heterozygous mutation or deletion of the *Zfhx1b* (*ZEB2, SIP1*) and is characterized by a distinctive facial appearance, intellectual disability, and variable other features including seizures, agenesis of the corpus callosum, and Hirschsprung disease (Mowat et al., 2003). Given *Zfhx1b*'s critical role in cortical interneuron development, we propose that cortical interneuron defects contribute to the seizure phenotype of MWS. Furthermore, since *Dlx1&2* regulate *Zfhx1b* expression in the subpallium, and *Dlx1&2* also regulate craniofacial and enteric nervous system development (Qiu et al., 1995) it will be intriguing whether *Zfhx1b* is also downstream of *Dlx* function during development of these tissues.

EXPERIMENTAL PROCEDURES

See Supplemental Experimental Procedures for detailed description of methods.

Mice

Zfhx1b $^{F/F}$ mice were genotyped according to (Miyoshi et al., 2006). *CAG-CAT-eGFP* mice were genotyped according to (Kawamoto et al., 2000). *Zfhx1b* $^{F/F}$ males were crossed to *Beta-Actin Cre* mice (Lewandoski et al., 1997) to generate the *Zfhx1b* null allele, which was followed by a cross to wild-type mice to eliminate the *Beta-Actin Cre* allele. *Zfhx1b*$^{+/-}$ mice were crossed with *Nkx2.1-Cre* or *I1/2b-Cre* mice, and male *Zfhx1b*$^{+/-}$; *Cre*$^{+}$ mice were crossed with female *Zfhx1b*$^{F/F}$ mice with or without the *CAG-CAT-EGFP* allele to generate conditional mutant embryos. Animals were treated in accordance with the protocols approved by the NICHD and UCSF Animal Use Committee.

Histochemistry

Embryonic and postnatal brains were prepared and immunostained (Flandin et al., 2010) or assayed by in situ hybridization (Jeong et al., 2008). Protocols can be found on our lab website http://physio.ucsf.edu/rubenstein/protocols/index.asp, with modifications for dual immuno/in situ fluorescence analysis described in the Supplemental Experimental Procedures.

Cell Culture, Transfections, and Luciferase Assays

P19 cells were cultured as described in (Farah et al., 2000). Experimental conditions were tested in triplicate by transfection of cells in 12-well plates using Fugene 6 (Roche). Cotransfection of a Renilla luciferase expression construct was used as a normalization control for a dual-luciferase assay. The following amounts of DNA were used in each well: 80 ng *pGL4.73* (Renilla Luciferase, Promega), 240 ng *pCAGGs-empty* or *pCAGGS-Dlx2*, 240ng *pGL4.23-empty* (Luciferase, Promega), or *pGL4.23-enhancer*. Luciferase and Renilla Luciferase quantification was done using a Promega Dual-Lucifase Assay Kit and a microplate luminometer (Veritas). Chi-square test showed that the levels of activation were significant *: $p < 0.05$.

Chromatin Immunoprecipitation (ChIP)

ChIP was performed similar to a published method (McKenna et al., 2011) with modifications described in Supplemental Experimental Procedures.

SUPPLEMENTAL INFORMATION

Supplemental Information includes six figures, three tables, and Supplemental Experimental Procedures and can be found with this article online at http://dx.doi.org/10.1016/j.neuron.2012.11.035.

ACKNOWLEDGMENTS

This work was supported by the research grants to J.L.R.R. from Nina Ireland, Weston Havens Foundation, Genentech, NIMH R37 MH049428 and R01 MH081880; to G.L.M. from Predoctoral Training in Neurobiology T32 GM007449; to L.A.P. and A.V. from NINDS R01NS062859A and NHGRI R01HG003988.; to G.L.M. from Predoctoral Training in Neurobiology T32 GM007449. L.A.P. and A.V. conducted research at the E.O. Lawrence Berkeley National Laboratory, performed under DOE DE-AC02-05CH11231, University of California. D.H. is funded by Queen Elisabeth Medical Foundation (1113), Scientific Research-Flanders (G.0954.11N), Research Council University of Leuven GOA, InfraMouse Hercules, and Belspo IUAP7/07. We thank Professor Melinda Duncan at the University of Delaware for providing *Zfhx1b*$^{F/+}$ mice.

Accepted: November 28, 2012
Published: January 9, 2013

REFERENCES

Anderson, S.A., Eisenstat, D.D., Shi, L., and Rubenstein, J.L. (1997a). Interneuron migration from basal forebrain to neocortex: dependence on Dlx genes. Science *278*, 474–476.

Anderson, S.A., Qiu, M., Bulfone, A., Eisenstat, D.D., Meneses, J., Pedersen, R., and Rubenstein, J.L. (1997b). Mutations of the homeobox genes Dlx-1 and Dlx-2 disrupt the striatal subventricular zone and differentiation of late born striatal neurons. Neuron *19*, 27–37.

Ardelt, A.A., Karpitskiy, V.V., Krause, J.E., and Roth, K.A. (1996). The neostriatal mosaic: basis for the changing distribution of neurokinin-1 receptor immunoreactivity during development. J. Comp. Neurol. *376*, 463–475.

Azim, E., Jabaudon, D., Fame, R.M., and Macklis, J.D. (2009). SOX6 controls dorsal progenitor identity and interneuron diversity during neocortical development. Nat. Neurosci. *12*, 1238–1247.

Batista-Brito, R., Machold, R., Klein, C., and Fishell, G. (2008). Gene expression in cortical interneuron precursors is prescient of their mature function. Cereb. Cortex *18*, 2306–2317.

Brown, K.N., Chen, S., Han, Z., Lu, C.-H., Tan, X., Zhang, X.-J., Ding, L., Lopez-Cruz, A., Saur, D., Anderson, S.A., et al. (2011). Clonal production and organization of inhibitory interneurons in the neocortex. Science *334*, 480–486.

Butt, S.J.B., Cobos, I., Golden, J., Kessaris, N., Pachnis, V., and Anderson, S. (2007). Transcriptional regulation of cortical interneuron development. J. Neurosci. *27*, 11847–11850.

Butt, S.J.B., Sousa, V.H., Fuccillo, M.V., Hjerling-Leffler, J., Miyoshi, G., Kimura, S., and Fishell, G. (2008). The requirement of Nkx2-1 in the temporal specification of cortical interneuron subtypes. Neuron *59*, 722–732.

Chen, Y., Wu, H., Wang, S., Koito, H., Li, J., Ye, F., Hoang, J., Escobar, S.S., Gow, A., Arnett, H.A., et al. (2009). The oligodendrocyte-specific G protein–coupled receptor GPR17 is a cell-intrinsic timer of myelination. Nat. Neurosci. *12*, 1398–1406.

Chen, L., Chatterjee, M., and Li, J.Y.H. (2010). The mouse homeobox gene Gbx2 is required for the development of cholinergic interneurons in the striatum. J. Neurosci. *30*, 14824–14834.

Chesselet, M.F., and Graybiel, A.M. (1986). Striatal neurons expressing somatostatin-like immunoreactivity: evidence for a peptidergic interneuronal system in the cat. Neuroscience *17*, 547–571.

Cobos, I., Long, J.E., Thwin, M.T., and Rubenstein, J.L. (2006). Cellular patterns of transcription factor expression in developing cortical interneurons. Cereb. Cortex *16(Suppl 1)*, i82–i88.

Cordes, S.P., and Barsh, G.S. (1994). The mouse segmentation gene *kr* encodes a novel basic domain-leucine zipper transcription factor. Cell *79*, 1025–1034.

Farah, M.H., Olson, J.M., Sucic, H.B., Hume, R.I., Tapscott, S.J., and Turner, D.L. (2000). Generation of neurons by transient expression of neural bHLH proteins in mammalian cells. Development *127*, 693–702.

Faux, C., Rakic, S., Andrews, W., Yanagawa, Y., Obata, K., and Parnavelas, J.G. (2009). Differential gene expression in migrating cortical interneurons during mouse forebrain development. J Comp. Neurol. *518*, 1232–1248.

Ferrón, S.R., Charalambous, M., Radford, E., McEwen, K., Wildner, H., Hind, E., Morante-Redolat, J.M., Laborda, J., Guillemot, F., Bauer, S.R., et al. (2011). Postnatal loss of Dlk1 imprinting in stem cells and niche astrocytes regulates neurogenesis. Nature *475*, 381–385.

Flandin, P., Kimura, S., and Rubenstein, J.L.R. (2010). The progenitor zone of the ventral medial ganglionic eminence requires Nkx2-1 to generate most of the globus pallidus but few neocortical interneurons. J. Neurosci. *30*, 2812–2823.

Flandin, P., Zhao, Y., Vogt, D., Jeong, J., Long, J., Potter, G., Westphal, H., and Rubenstein, J.L. (2011). Lhx6 and Lhx8 coordinately induce neuronal expression of Shh that controls the generation of interneuron progenitors. Neuron *70*, 939–950.

Fragkouli, A., van Wijk, N.V., Lopes, R., Kessaris, N., and Pachnis, V. (2009). LIM homeodomain transcription factor-dependent specification of bipotential MGE progenitors into cholinergic and GABAergic striatal interneurons. Development *136*, 3841–3851.

Gelman, D.M., and Marín, O. (2010). Generation of interneuron diversity in the mouse cerebral cortex. Eur. J. Neurosci. *31*, 2136–2141.

Gerstner, J.R., and Landry, C.F. (2007). Expression of the transcriptional coactivator CITED1 in the adult and developing murine brain. Dev. Neurosci. *29*, 203–212.

Higashi, Y., Maruhashi, M., Nelles, L., Van de Putte, T., Verschueren, K., Miyoshi, T., Yoshimoto, A., Kondoh, H., and Huylebroeck, D. (2002). Generation of the floxed allele of the SIP1 (Smad-interacting protein 1) gene for Cre-mediated conditional knockout in the mouse. Genesis *32*, 82–84.

Jen, Y.-H.L., Musacchio, M., and Lander, A.D. (2009). Glypican-1 controls brain size through regulation of fibroblast growth factor signaling in early neurogenesis. Neural Dev. *4*. http://dx.doi.org/10.1186/1749-8104-4-33.

Jeong, J., Li, X., McEvilly, R.J., Rosenfeld, M.G., Lufkin, T., and Rubenstein, J.L.R. (2008). Dlx genes pattern mammalian jaw primordium by regulating both lower jaw-specific and upper jaw-specific genetic programs. Development *135*, 2905–2916.

Kawamoto, S., Niwa, H., Tashiro, F., Sano, S., Kondoh, G., Takeda, J., Tabayashi, K., and Miyazaki, J. (2000). A novel reporter mouse strain that expresses enhanced green fluorescent protein upon Cre-mediated recombination. FEBS Lett. *470*, 263–268.

Lavdas, A.A., Grigoriou, M., Pachnis, V., and Parnavelas, J.G. (1999). The medial ganglionic eminence gives rise to a population of early neurons in the developing cerebral cortex. J. Neurosci. *19*, 7881–7888.

Lewandoski, M., Meyers, E.N., and Martin, G.R. (1997). Analysis of Fgf8 gene function in vertebrate development. Cold Spring Harb. Symp. Quant. Biol. *62*, 159–168.

Liodis, P., Denaxa, M., Grigoriou, M., Akufo-Addo, C., Yanagawa, Y., and Pachnis, V. (2007). Lhx6 activity is required for the normal migration and specification of cortical interneuron subtypes. J. Neurosci. *27*, 3078–3089.

Long, J.E., Cobos, I., Potter, G.B., and Rubenstein, J.L.R. (2009a). Dlx1&2 and Mash1 transcription factors control MGE and CGE patterning and differentiation through parallel and overlapping pathways. Cereb. Cortex *19*(*Suppl 1*), i96–i106.

Long, J.E., Swan, C., Liang, W.S., Cobos, I., Potter, G.B., and Rubenstein, J.L.R. (2009b). Dlx1&2 and Mash1 transcription factors control striatal patterning and differentiation through parallel and overlapping pathways. J. Comp. Neurol. *512*, 556–572.

Lu, Q.R., Yuk, D., Alberta, J.A., Zhu, Z., Pawlitzky, I., Chan, J., McMahon, A.P., Stiles, C.D., and Rowitch, D.H. (2000). Sonic hedgehog-regulated oligodendrocyte lineage genes encoding bHLH proteins in the mammalian central nervous system. Neuron *25*, 317–329.

Maira, M., Long, J.E., Lee, A.Y., Rubenstein, J.L.R., and Stifani, S. (2010). Role for TGF-beta superfamily signaling in telencephalic GABAergic neuron development. J. Neurodev. Disord. *2*, 48–60.

Marin, O., Anderson, S.A., and Rubenstein, J.L. (2000). Origin and molecular specification of striatal interneurons. J. Neurosci. *20*, 6063–6076.

Marín, O., Yaron, A., Bagri, A., Tessier-Lavigne, M., and Rubenstein, J.L. (2001). Sorting of striatal and cortical interneurons regulated by semaphorin-neuropilin interactions. Science *293*, 872–875.

McKenna, W.L., Betancourt, J., Larkin, K.A., Abrams, B., Guo, C., Rubenstein, J.L.R., and Chen, B. (2011). Tbr1 and Fezf2 regulate alternate corticofugal neuronal identities during neocortical development. J. Neurosci. *31*, 549–564.

Miquelajauregui, A., Van De Putte, T., Polyakov, A., Nityanandam, A., Boppana, S., Seuntjens, E., Karabinos, A., Higashi, Y., Huylebroeck, D., and Tarabykin, V. (2007). Smad-interacting protein-1 (Zfhx1b) acts upstream of Wnt signaling in the mouse hippocampus and controls its formation. Proc. Natl. Acad. Sci. USA *104*, 12919–12924.

Miyoshi, T., Maruhashi, M., Van De Putte, T., Kondoh, H., Huylebroeck, D., and Higashi, Y. (2006). Complementary expression pattern of Zfhx1 genes Sip1 and deltaEF1 in the mouse embryo and their genetic interaction revealed by compound mutants. Dev. Dyn. *235*, 1941–1952.

Moon, Y.S., Smas, C.M., Lee, K., Villena, J.A., Kim, K.-H., Yun, E.J., and Sul, H.S. (2002). Mice lacking paternally expressed Pref-1/Dlk1 display growth retardation and accelerated adiposity. Mol. Cell Biol. *22*, 5585–5592.

Mowat, D.R., Wilson, M.J., and Goossens, M. (2003). Mowat-Wilson syndrome. J. Med. Genet. *40*, 305–310.

Nóbrega-Pereira, S., Kessaris, N., Du, T., Kimura, S., Anderson, S.A., and Marín, O. (2008). Postmitotic Nkx2-1 controls the migration of telencephalic interneurons by direct repression of guidance receptors. Neuron *59*, 733–745.

Nobrega-Pereira, S., Gelman, D., Bartolini, G., Pla, R., Pierani, A., and Marin, O. (2010). Origin and molecular specification of globus pallidus neurons. J. Neurosci. *30*, 2824–2834.

Petryniak, M.A., Potter, G.B., Rowitch, D.H., and Rubenstein, J.L.R. (2007). Dlx1 and Dlx2 control neuronal versus oligodendroglial cell fate acquisition in the developing forebrain. Neuron *55*, 417–433.

Potter, G.B., Petryniak, M.A., Shevchenko, E., Mckinsey, G.L., Ekker, M., and Rubenstein, J.L.R. (2008). Generation of Cre-transgenic mice using Dlx1/Dlx2 enhancers and their characterization in GABAergic interneurons. Mol. Cell. Neurosci. *40*, 167–186.

Qiu, M., Bulfone, A., Martinez, S., Meneses, J.J., Shimamura, K., Pedersen, R.A., and Rubenstein, J.L. (1995). Null mutation of Dlx-2 results in abnormal morphogenesis of proximal first and second branchial arch derivatives and abnormal differentiation in the forebrain. Genes Dev. *9*, 2523–2538.

Rudy, B., Fishell, G., Lee, S., and Hjerling-Leffler, J. (2011). Three groups of interneurons account for nearly 100% of neocortical GABAergic neurons. Dev. Neurobiol. *71*, 45–61.

Sánchez-Alcañiz, J.A., Haege, S., Mueller, W., Pla, R., Mackay, F., Schulz, S., López-Bendito, G., Stumm, R., and Marín, O. (2011). Cxcr7 controls neuronal migration by regulating chemokine responsiveness. Neuron *69*, 77–90.

Sanchez-Ortiz, E., Yui, D., Song, D., Li, Y., Rubenstein, J.L., Reichardt, L.F., and Parada, L.F. (2012). TrkA gene ablation in basal forebrain results in dysfunction of the cholinergic circuitry. J. Neurosci. *32*, 4065–4079.

Seuntjens, E., Nityanandam, A., Miquelajauregui, A., Debruyn, J., Stryjewska, A., Goebbels, S., Nave, K.-A., Huylebroeck, D., and Tarabykin, V. (2009). Sip1 regulates sequential fate decisions by feedback signaling from postmitotic neurons to progenitors. Nat. Neurosci. *12*, 1373–11380.

Sussel, L., Marin, O., Kimura, S., and Rubenstein, J.L. (1999). Loss of Nkx2.1 homeobox gene function results in a ventral to dorsal molecular respecification within the basal telencephalon: evidence for a transformation of the pallidum into the striatum. Development *126*, 3359–3370.

Tepper, J.M., Tecuapetla, F., Koós, T., and Ibáñez-Sandoval, O. (2010). Heterogeneity and Diversity of striatal GABAergic interneurons. Front. Neuroanat. *4*. http://dx.doi.org/10.3389/fnana.2010.00150.

van Grunsven, L.A., Michiels, C., Van De Putte, T., Nelles, L., Wuytens, G., Verschueren, K., and Huylebroeck, D. (2003). Interaction between Smad-interacting protein-1 and the corepressor C-terminal binding protein is dispensable for transcriptional repression of E-cadherin. J. Biol. Chem. *278*, 26135–26145.

van den Berghe, V., Stappers, E., Vandesande, B., Dimidschstein, J., Kroes, R., Francis, A., Conidi, A., Lesage, F., Dries, R., Cazzola, C., et al. (2012). Directed migration of cortical interneurons depends on the cell-autonomous action of Sip1. Neuron *77*, this issue, 70–82.

Vandewalle, C., Van Roy, F., and Berx, G. (2009). The role of the ZEB family of transcription factors in development and disease. Cell. Mol. Life Sci. *66*, 773–787.

Verschueren, K., Remacle, J.E., Collart, C., Kraft, H., Baker, B.S., Tylzanowski, P., Nelles, L., Wuytens, G., Su, M.T., and Bodmer, R. (1999). SIP1, a novel zinc finger/homeodomain repressor, interacts with Smad proteins and binds to 5′-CACCT sequences in candidate target genes. J. Biol. Chem. *274*, 20489–20498.

Verstappen, G., Van Grunsven, L.A., Michiels, C., Van De Putte, T., Souopgui, J., Van Damme, J., Bellefroid, E., Vandekerckhove, J., and Huylebroeck, D. (2008). Atypical Mowat-Wilson patient confirms the importance of the novel association between ZFHX1B/SIP1 and NuRD corepressor complex. Hum. Mol. Genet. *17*, 1175–1183.

Visel, A., Minovitsky, S., Dubchak, I., and Pennacchio, L.A. (2007). VISTA Enhancer Browser–a database of tissue-specific human enhancers. Nucleic Acids Res. *35*, D88–D92.

Visel, A., Prabhakar, S., Akiyama, J.A., Shoukry, M., Lewis, K.D., Holt, A., Plajzer-Frick, I., Afzal, V., Rubin, E.M., and Pennacchio, L.A. (2008). Ultraconservation identifies a small subset of extremely constrained developmental enhancers. Nat. Genet. *40*, 158–160.

Wang, S., Sdrulla, A., Johnson, J.E., Yokota, Y., and Barres, B.A. (2001). A role for the helix-loop-helix protein Id2 in the control of oligodendrocyte development. Neuron *29*, 603–614.

Wang, Y., Li, G., Stanco, A., Long, J.E., Crawford, D., Potter, G.B., Pleasure, S.J., Behrens, T., and Rubenstein, J.L.R. (2011). CXCR4 and CXCR7 have distinct functions in regulating interneuron migration. Neuron *69*, 61–76.

Xu, Q., Tam, M., and Anderson, S.A. (2008). Fate mapping Nkx2.1-lineage cells in the mouse telencephalon. J. Comp. Neurol. *506*, 16–29.

Yun, K., Fischman, S., Johnson, J., Hrabe de Angelis, M., Weinmaster, G., and Rubenstein, J.L.R. (2002a). Modulation of the notch signaling by Mash1 and Dlx1/2 regulates sequential specification and differentiation of progenitor cell types in the subcortical telencephalon. Development *129*, 5029–5040.

Yun, K., Mantani, A., Garel, S., Rubenstein, J., and Israel, M.A. (2004). Id4 regulates neural progenitor proliferation and differentiation in vivo. Development *131*, 5441–5448.

Zhao, Y., Marín, O., Hermesz, E., Powell, A., Flames, N., Palkovits, M., Rubenstein, J.L.R., and Westphal, H. (2003). The LIM-homeobox gene Lhx8 is required for the development of many cholinergic neurons in the mouse forebrain. Proc. Natl. Acad. Sci. USA *100*, 9005–9010.

Zhao, Y., Flandin, P., Long, J.E., Cuesta, M.D., Westphal, H., and Rubenstein, J.L.R. (2008). Distinct molecular pathways for development of telencephalic interneuron subtypes revealed through analysis of Lhx6 mutants. J. Comp. Neurol. *510*, 79–99.

厚生労働科学研究費補助金

障害者対策総合研究事業（神経・筋疾患分野）

下部神経管閉鎖障害の病態・制御研究

平成24年度　総括･分担研究報告書

発行　　平成25年4月

発行所　下部神経管閉鎖障害の病態・制御研究班事務局
名古屋大学大学院医学系研究科神経遺伝情報学分野
〒466-8550　名古屋市昭和区鶴舞町65
TEL: 052-744-2447　FAX: 052-744-2449